Applied Scientific Research **54:** 349–385, 1995.

Coherent Structures and Riblets

SEDAT F. TARDU
Laboratoire des Ecoulements Géophysiques et Industriels, Institut de Mécanique de Grenoble, CNRS-UJF-INPG, BP 53-X 38041, Grenoble Cédex, France

Received 10 May 1994; accepted in revised form 30 April 1995

Abstract. This work deals with the effect of the riblets on the coherent structures near the wall. The emphasis is put on the genesis of the quasi-streamwise vortices in the presence of the riblets. The quasi-streamwise vortices regenerate by the tilting of wall normal vorticity induced by prevailing structures. This requires a mechanism which leads to a temporal streamwise dependence near the elongated flow structures and to a subsequent formation of new wall normal vorticity. It is suggested here that the action of existing quasi-streamwise vortices on the sidewalls of wall normal vorticity may create a local, streamwise dependent spanwise velocity and therefore, a secondary wall normal vorticity field. A preliminary analysis of the set-up and the time and space development of this secondary three-dimensional flow associated with the regeneration mechanism, is given. An attempt is made, in order to explain the drag reduction performed by the riblets through an intermittent model, based on the protrusion height. Logical estimates of the amount of drag reduction are obtained. The differences between the mechanism suggested here and those based on forced control experiments are also discussed.

Key words: near wall turbulence, regeneration of the quasi-streamwise vortices (QSV), set-up of three dimensionality near the QSVs, effect of the riblets, forced control experiments

1. Introduction

The research devoted to the mechanism of drag reduction performed by the riblets is confronted to the slight alteration of flow structures generating the wall shear stress. In addition to that, this effect is localized in a thin region near the wall. The experimental work is tremendously delicate in these circumstances. That partly explains the discrepancies found in the published results concerning the fine structure of the near wall turbulence in riblets mounted boundary layers (see for example Tardu et al. [39] for a short review on the bursting process). One has to add to these complexities our lack of clear understanding in the kinematics and dynamics of the turbulence producing eddies even, in the simple canonical flat plate case.

Most of the existing experimental data deals with the modifications of the structures related to the streamwise flow. This is probably, because, these quantities are easier to measure, but, also because the importance of the cross flow in the genesis of the near wall structures has only recently been discovered [6, 34]. For the past few years, the differences in the reaction of the streamwise and cross viscous Stokes flows in the presence of the riblets have been well known [2, 23]. The virtual origin of the viscous spanwise velocity is higher than that of the streamwise velocity

in drag reducing configurations. Until now, this characteristic has been interpreted as being the capacity of the riblets geometry to impede the instantaneous cross flow more than the longitudinal one and to reduce "the whole turbulent momentum exchange" ([2], p. 125). The drag reduction, in return, is explained by a more important resistance to the cross flow because its virtual origin penetrates further into the flow [23]. However, at the present time the consequence of this phenomena on the wall shear stress producing eddies is unclear. It is widely accepted by now, that the elongated quasi-streamwise vortices (or one-legged hairpins) are the dominant feature of the inner layer [33]. On the other hand, there is a close relationship between the existence of these structures and the generation of the drag. The passive or active control of the former, depends upon the intervention, either directly on the quasi-streamwise vortices, or indirectly on their interaction with the near wall flow. Curiously, the genesis of the streamwise vorticity layers is intimately related to the cross flow. The question asked here, is how is the process of regeneration of active structures modified by the riblets.

This work focuses on the near wall vorticity dynamics in the canonical and manipulated turbulent boundary layers. A short review on the spatio-temporal reaction of the near wall turbulence to the riblets is given in Section 2. This is further developed in Section 3 wherein it is attempted to explain the relative stability of the flow within the ribs when there is decrease of drag. A conceptual model of the regeneration of the quasi-streamwise vortices is proposed in Section 4. An intermittent mechanism which leads to drag reduction is suggested in Section 5. Finally, some observations are made in Section 6, on the consequences of artificial and selective introduction of spanwise velocity at the wall which was recently used to model the riblets mounted boundary layer by Jiménez [19]. Some concluding remarks are made in the last section.

2. Summary of the Effect of the Riblets on the Near Wall Turbulence

2.1. Effect on the Spatio-Temporal Behaviour of the Near Wall Turbulence

The dynamic process which takes place within and near the riblets is of major importance in order to explain the mechanism of drag reduction. It is difficult to explore this process by means of experimentation. Carefully conducted one point measurements of the Reynolds shear stresses including quadrant decomposition within and immediately above the grooves exist but they are rare [4, 45, 46]. To the author's knowledge, the details of the vorticity fields are only available from the numerical simulations. There is a chance of experimental insight into the vorticity statistics by making use of the PIV as one of the referees has pointed out, but the author was not aware of such efforts when this paper was in preparation. The data obtained by direct simulations [8] and 2 1/2 models [42, 43] indicate an important decrease in the intensity of the streamwise and spanwise vorticity fluctuations, showing that the streamwise vortices responsible for the bursting near the wall are

weakened in the presence of the riblets. It seems that there is a reasonable link between the decrease of the streamwise vorticity fluctuations $\omega_x' = \sqrt{\overline{\omega_x \omega_x}}$ and the observed trend of the bursting frequency of Tardu et al. [39] (Fig. 1a). The decrease of the spanwise vorticity intensity is also interesting and may indicate that the vorticity associated with the legs of the hairpin vortices is lower. Consequently, the lateral expansion of the near wall structures is also weakened by the presence of the riblets as suggested by Walker [47]. Note however that, in a drag increasing configuration the spanwise vorticity fluctuations decrease above the riblet valley, as in a drag reducing case [8]. The increase in ω_z' above the riblet tip however, is quite significant and dominates the near wall dynamics.

The increase of the flatness of streamwise velocity fluctuations related to the intermittence is a well-known characteristic of the riblets sublayer [7]. The high order statistics of the time derivative of streamwise velocity fluctuations $\mathrm{d}u'/\mathrm{d}t$ are even more interesting because they are more closely related to the vorticity mechanics near the wall. Tardu et al. [39] reported that the flatness $F_{\mathrm{d}u'/\mathrm{d}t}$ is significantly larger above the riblets compared with the standard boundary layer (Fig. 1b). The skewness $S_{\mathrm{d}u'/\mathrm{d}t}$ is in return unaffected. The former is qualitatively related to the production of the mean square vorticity by stretching, and provides a measure of the importance of non-linearity in the inner layer which is, therefore, only mildly sensitive to the riblets. Supposing that the Taylor hypothesis is valid, the increase of $F_{\mathrm{d}u'/\mathrm{d}t}$ indicates, in return, that the occurrence of the streamwise variations of the longitudinal velocity $\mathrm{d}u'/\mathrm{d}x$ is more intermittent in the manipulated boundary layer. This is in agreement with Chu and Karinidakis [9] who observed that the streamwise motion of the near wall structures is less wavy in the riblets sublayer. This point, together with the set-up of the undulatory motion of the structures during the regeneration cycle are deferred to Section 4.

2.2. Effect on the spatial extent of the near wall structures

An increase in the spanwise extent of near wall structures obtained either by long time spanwise correlation distributions at zero time delay [13], by conditional correlation measurements [7] or by visual counting [1] is commonly reported by several authors. The increase in the size of the eddies is consistent with the drag reduction mechanism suggested by Lumley and Kubo [25]. These authors argue that the quasi-streamwise vortices near the wall negotiate the sharp peaks of the riblets by growing larger. Such an increase is also predicted by the recent conceptual model of Jiménez [19] which shall be discussed at length in this paper.

There are just as many studies indicating that the sizes of the structures are unaffected by the riblets. For instance, the flow visualisations of Hooshmand et al. [15] showed no apparent differences in the average spacing between structures. The interesting point they reported concerns the capacity of the riblets to constrain the flow marker within the ribs and to weaken the interaction between the adjacent

a

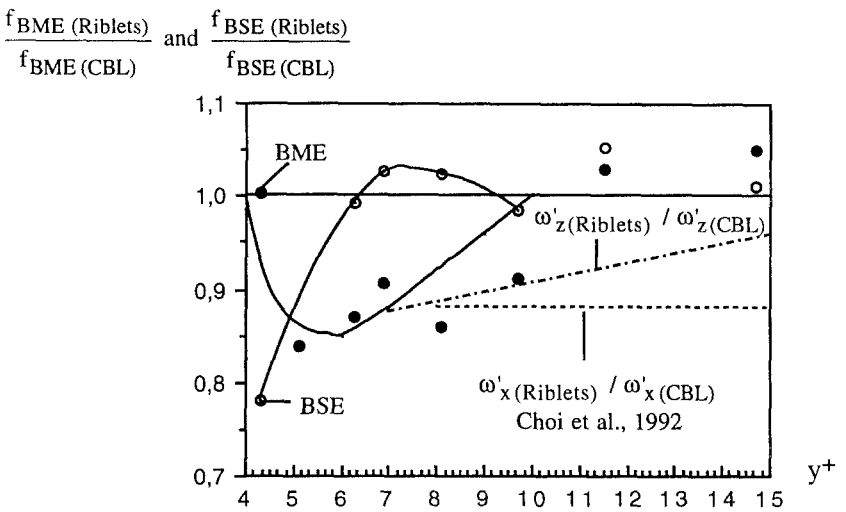

b

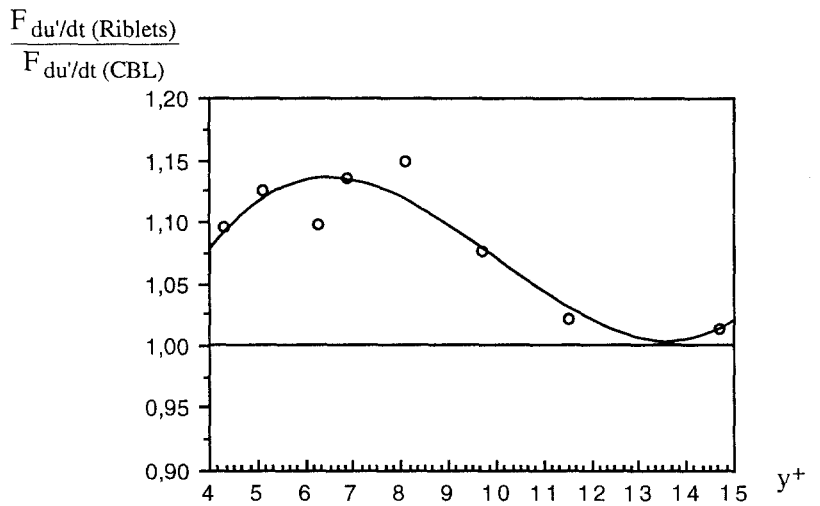

Fig. 1. (a) Distribution of the bursting frequency [39] and the rms of the streamwise and spanwise vorticity fluctuations ([8], Figure 14). BME and BSE refers to respectively to the burst with multiple and single ejections. The subindices Riblets and CBL designate the manipulated (by the riblets) and canonical boundary layers. The origin in y^+ is the tip of the riblets and the friction velocity on the smooth wall is used in the non-dimensionalization. (b) Flatness of du'/dt according to Tardu et al. [39].

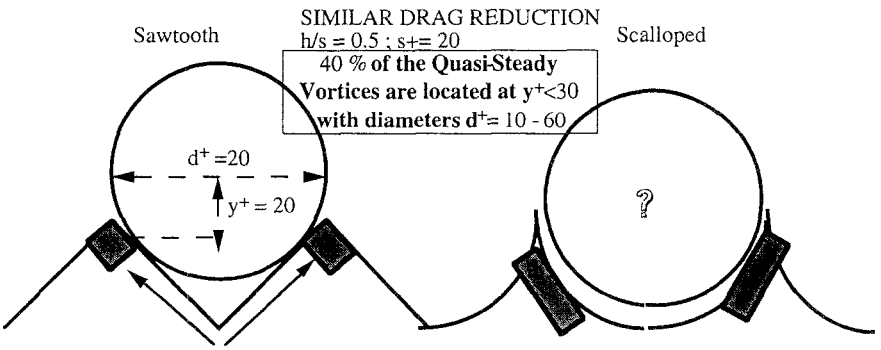

Fig. 2. Drag reduction mechanism suggested by Choi et al. [8].

grooves. This is one of the main effects of the drag reducing surface geometry as will be discussed in Section 4.

A further example of disagreement came recently from Choi et al. [8]. The results inferred from the direct numerical simulations (DNS) undertaken by these authors are along the same lines as Hooshmand et al. [15], in that the locations and sizes of the streamwise vortices are not drastically affected by the changes in surface geometry. Consequently, the drag reduction mechanism they propose is not based on the modifications of the sizes of the structures. They suggest that, when the riblets pitch is smaller than the average diameter of the quasi-streamwise vortices, the high skin friction they induce by sweep motions is limited to a smaller area near the tips (Fig. 2). This suggestion presents several shortcomings, even though it gives a reasonable estimate of the optimum riblets pitch which should not exceed the average diameter of the structures. This is rather a "geometrical approach". First of all, the drag reduction obtained with the scalloped riblets of similar sizes, can scarcely be explained by this model (Fig 2). Secondly, 40% of the quasi-streamwise vortices are located at $y^+ < 30$ with diameters $d^+ = 10$–60 [32, 33]; here, $(^+)$ stands for the quantities non-dimensionalized by the wall variables, i.e. the viscosity ν and the shear velocity u_τ). This indicates that the action of the smaller structures near the riblets may still be significant in a drag reducing configuration.

A quite different mechanism is proposed by Phillips [29–31]. This author argues that the riblets may excite the most unstable mode at Craik–Leibovich sense which has a spanwise wavelength of about 20–40 wall units, resulting in vortices smaller in diameter and confined to the buffer layer. This is a quite interesting point of view, but the present author found no evidence of such a mechanism in for example the DNS data of Chu and Karinidakis [9], and of Choi et al. [8].

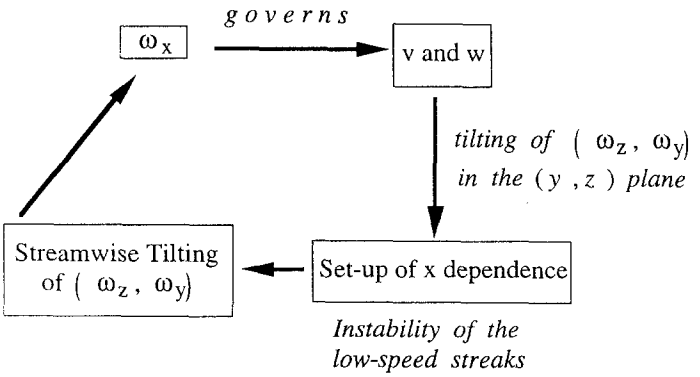

Fig. 3. Structure genesis following Jiménez and Moin [16].

3. New Developments in Near Wall Turbulence Research and Their Implications: Overall View

We will first summarize some of the mechanisms of the regeneration of near wall turbulence generating events revealed by recent studies. In this section, the accent is put on the behaviour of near wall transverse vortices and shear layers together with their interaction with the riblets. The genesis of the elongated streamwise structures is discussed in more detail in Sections 4 and 5.

Jiménez and Moin [16] studied the regeneration mechanism in the minimal flow unit necessary to sustain the turbulence. The dimensions of the unit are $\lambda_z^+ \approx 100$ in the spanwise and $\lambda_x^+ \approx 250$–350 in the streamwise directions. The first value is the streak spacing as expected and the second is the minimum streamwise distance of the active eddies. It is interesting to note that the former coincides reasonably well with the distance separating the ejections of clusters of events. Indeed the time interval between the multiple ejections is about $\Delta t^+ = 20$ at $y^+ = 15$ [40]. Using a convection velocity equal approximately to the local one U^+ this results in a streamwise distance between structures of $\Delta t^+ = 225$. Jiménez and Moin detailed the mechanism in the very near wall region because the minimum flow unit is incapable of modelling the outer flow structures. The basic elements of the process they suggested can be summarized as follows (Fig. 3):

- Most of the vorticity in the viscous sublayer is in the spanwise z-direction, and the stress producing quasi-streamwise vortices which are the basic structures in the inner layer ($10 < y^+ < 100$) originate from the tilting of the ω_z vortex lines.
- Very near the wall, the transverse instantaneous velocity components v and w are governed by the streamwise vorticity ω_x. Indeed, since in this region $\partial/\partial x \ll \partial/\partial z$ it can easily be shown that:

$$u \approx -\omega_z y; \quad v \approx -\frac{1}{2}\frac{\partial \omega_x}{\partial z} y^2 \quad \text{and} \quad w = y\omega_x.$$

- The prevailing transverse shear layers wherein the wall normal and spanwise vorticity (ω_y, ω_z) are concentrated at a given time are pushed away by (v, w) induced by the interaction of the quasi-streamwise vortices with the wall fluid.
- An x-dependence is necessary for the forward tilting of the (ω_y, ω_z) layers in the flow direction, to regenerate a new quasi-streamwise vortex and close the cycle. One has indeed:

$$\frac{D\omega_x}{Dt} = \omega_x \frac{\partial u}{\partial x} - \frac{\partial w}{\partial x}\frac{\partial u}{\partial y} + \frac{\partial v}{\partial x}\frac{\partial u}{\partial z} + \nu \nabla^2 \omega_x.$$

It is clear that without streamwise x-dependence, the stretching, tilting and twisting terms in the rate of change of ω_x vanish. In the viscous wall region, the largest contribution to the rate of change of the streamwise vorticity, is the tilting of ω_z with a net contribution of $-(\partial w/\partial x)(\partial u/\partial y)$ [6, 14]. The stretching of the existing streamwise vorticity and the twisting of the spanwise vorticity are of secondary importance. The induction of the x-dependence near the elongated streamwise structures should be somewhat related to their interaction with the wall flow, i.e. to the structures themselves in conformity with the "regeneration philosophy". This is not an easy task as will be discussed in Section 4. One point of view is that the three-dimensionality of the prevailing shear layer is set up by the undulatory motion of the low speed streaks associated with the inflectional instability due to the instantaneous spanwise variations $\partial u/\partial z$ of the fluctuating longitudinal velocity [14, 37].

The key elements are now present to interpret the weakening of the quasi-streamwise vortices and probably the presence of the weak secondary vortices near a drag-reducing riblet wall [1, 43]. Two suggestions may already be made, namely:

1. The riblets prevent and weaken the set-up of the three-dimensionality within the ribs by limiting the lateral motion of the z vorticity layer pushed away by a quasi-streamwise vortex as shown in Fig. 4. The author believes that the most pronounced effect of the riblets is presumably the shortening of the time period that the low speed streak instability requires to develop. In order to make an order of magnitude analysis of such a developing time, one needs an idea of the spanwise expansion rate of the z-vorticity layer. Taylor and Smith ([41], p. 93) have shown that the spanwise spreading rate of a typical hairpin structure* is about $\Delta z/\Delta x = 0.05$. That gives a typical spreading velocity of the vorticity layer of about:

$$v_{sz}^+ = \frac{\Delta z^+}{\Delta x^+}\frac{\Delta x^+}{\Delta t^+} = \frac{\Delta z^+}{\Delta x^+} u_c^+,$$

where u_c^+ is the convection velocity of the related structure. Since the convection velocity of the vortical structures is $u_c^+ = 10$ for $y^+ < 10$ [37], $v_{sz}^+ \approx 0.5$. In a drag

* The similarity between the regeneration mechanism studied here and the one-leg hairpin model is recalled (see [16], p. 235). The spreading rate of the z-vorticity should therefore be similar to the spanwise spreading rate of a similar hairpin structure.

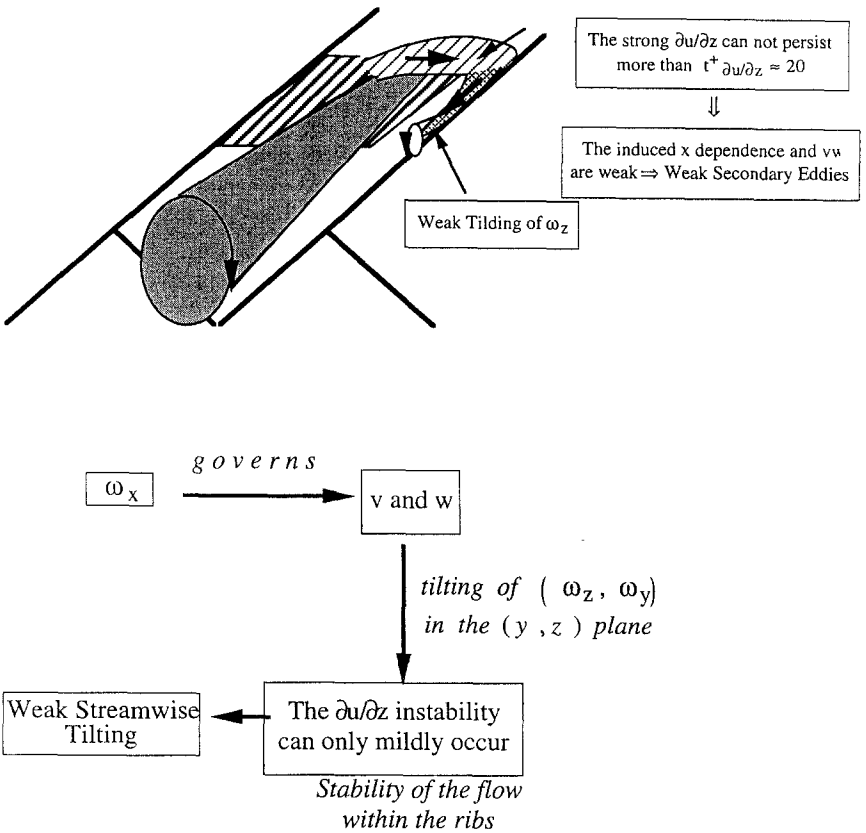

Fig. 4. Possible effect of a quasi-streamwise vortex on the flow near the riblets.

reducing configuration and when a quasi-streamwise vortex is within the groove with the width typically $s^+ = 12$, the time of the set-up of the spanwise instability is about $t^+_{\partial u/\partial z} = s^+/v^+_{sz} \approx 20$. The governing instability can therefore persist only up to 20 wall units and this is significantly smaller than $t^+_{\partial u/\partial z} = 60$ reported by Swearingen et al. ([37], p. 295) in the canonical boundary layer. Jiménez and Moin [16] also report that the lifting of the wall vorticity and the subsequent deviation from the two-dimensionality is a slow process which requires a time interval of about 100 wall units (Fig. 25, p. 235 of their paper). Note that in a drag increasing configuration with large riblet spacing $s^+ = 40$, the set-up time is large enough to regenerate new structures within the ribs, enhance the momentum exchange and eventually increase the drag. Consequently and although there is no reason that smaller quasi-streamwise vortices can interact with the flow within the ribs, the induced streamwise tilting of the wall vorticity layers necessary to regenerate new streamwise structures can only mildly occur in this region. The lift-up vorticity layer can also be weakened by strong viscous dissipation as it develops from one to the adjacent tops of the ribs [38] reducing the regeneration of adjacent v and

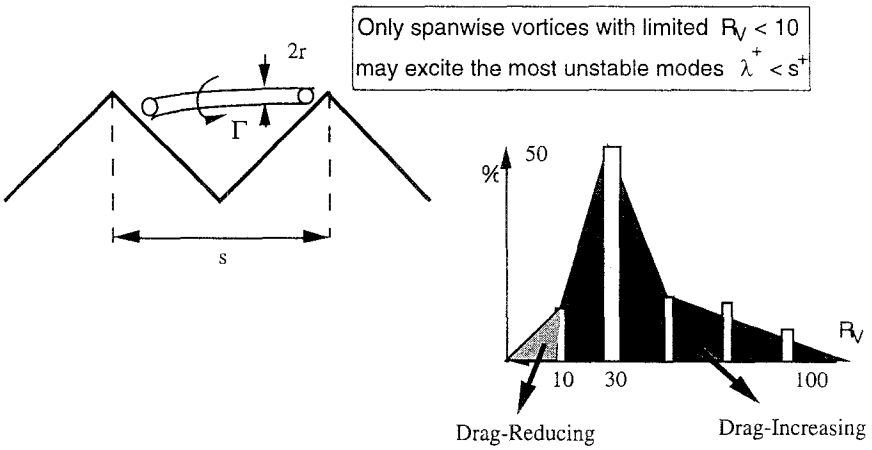

Fig. 5. A spanwise vortex filament on the riblet surface and the set-up of instability.

w velocities. This seems to explain the remarkable stability of the flow within the riblets and their capacity of "accumulating slow flow in the riblet grooves" reported by several authors [42, 43, 48]. Small quasi-streamwise vortices can however still be generated because of the strong shear present near the tips as shown in Fig. 4, but these structures are probably less significant.

Swearingen et al. [37] have shown that the undulation of the low speed streaks occur simultaneously with strong quadrant 1 and quadrant 4 vw events prior to the break up into chaotic motion. This mechanism is similar in every aspect to the one detailed by Brooke and Hanratty [6] and Bernard et al. [5]. The former indicated that the new quasi-streamwise vortices are born in time when the x-vorticity is enhanced by the tilting of wall normal ω_y vorticity through $-(\partial w/\partial x)(\partial u/\partial y)$, i.e. when the tilting causes a large decrease or increase of the instantaneous spanwise velocity w in the flow direction. This phenomena which is rather newly observed, indicates that the drag is mainly governed by the control of this term. In a drag increasing configuration for which the birth process may eventually occur in the riblets valley, the set-up of high cross-flow velocities may generate strong secondary riblet eddies as observed by several authors (for example [43]).

Consider now the effect of a spanwise vortex filament on the riblet surface (Fig. 5). Kawahara et al. [20] studied the long-wavelength instability of a rectilinear vortex in a background shear. They have shown that the spanwise vortex filament is unstable (and regenerates quasi-streamwise vortices) when:

$$\beta = -\frac{r^{+2}}{2R_V} > 0,$$

where r^+ is the radius of the vortex in wall units and R_V is its Reynolds number $R_V = \Gamma/2\pi\nu$ (with Γ being the associated circulation). The physical interpretation of this relationship is the set-up of instability when the stabilizing effect of the self-induced rotation is opposite to the background rotation. By using the distribution

of the diameter and the Re number of the spanwise vortices given by Robinson [33], Kawahara et al. [20] have shown that the most unstable wavelength λ is close to the streak spacing. At $y^+ = 5$ for instance, $\lambda^+ = 60$ and it is interesting to note that $\lambda^+ \approx s^+$ in a drag increasing configuration in which the instability may freely develop. According to these results, it may be suggested that the riblets inhibit the break-up of the spanwise vortex filaments tip to tip which eventually leads to weak quasi-streamwise vortices in the valley. Consider indeed those spanwise vortices which are embedded between the ribs and are potentially capable of enhancing streamwise vortices. In order that such a process takes place, the most unstable spanwise wavelength of the transverse vortex has to be limited by the width of the riblets i.e. $\lambda^+ < s^+$. Considering that the vortex diameters are still a linear function of y^+ i.e. $r^+ = \frac{1}{2} > \kappa y^+$ (with κ the Karman constant) in the same way as in the canonical boundary layer (CBL hereafter) that results in:

$$k^+ r^+ \geq \pi\kappa \frac{y^+}{s^+}$$

and

$$\beta = \frac{\kappa^2}{8} \frac{y^{2+}}{\mathrm{R}_V} .$$

Following Kawahara et al. ([20], p. 406, Fig. 2) the maximum instability for a fixed β is approximately linear until $k^+ r^+ = 1$ with $\beta \approx \frac{1}{3} > k^+ r^+$. Combining these relationships, the upper limit of the Re number associated with an unstable vortex is $\mathrm{R}_V \leq 0.05 y^+ s^+ \approx 0.05 s^{+2}$. For a drag reducing case with typically $s^+ = 15$, that results in $\mathrm{R}_V < 10$ which is small compared with the mean Reynolds number $\mathrm{R}_V = 30$ of the spanwise vortices in a CBL and which consequently leads to smaller growth rates (Fig. 5). This quite crude model could be an indication of the presence of weak quasi-streamwise vortices within the ribs. This approach is however open to several criticisms, firstly because the estimation is based on CBL and secondly in the region which is investigated here the transverse vortices are only occasionally present.

2. In the riblet's buffer layer the regeneration mechanism is active and the set-up of streamwise dependence through the wall normal vorticity takes place in a manner similar to the CBL. Since, "significant spanwise variations of the vorticity fluctuations occur only near the riblets" ([8], p. 15) in a drag decreasing configuration, it is expected that the birth of new structures occurs in a more localized fashion compared with drag increasing configuration for which there is further penetration of the ω_x, ω_y, ω_z distributions into the channel.

It is expected that in this region the riblets do not drastically reduce the number of active events but alter their strengths by interactions between the naturally existing structures and the secondary eddies induced near the ribs. A possible scenario is given in Fig. 6. Since there is no limitation to the streamwise development of the flow, it is not expected that the tilting of ω_y will be drastically affected in this

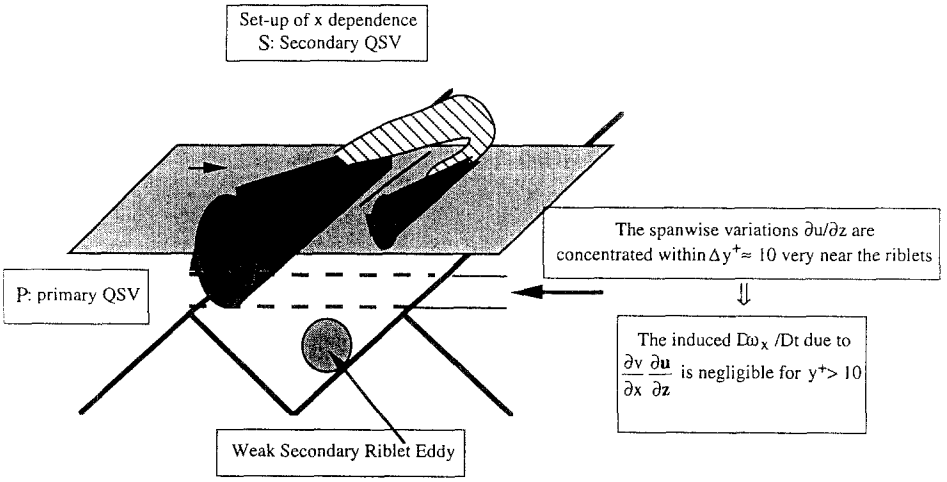

Fig. 6. Effect on the quasi-streamwise vortices in the riblet's buffer layer.

region. What should be expected on the contrary is a mitigation of wall normal vorticity ω_y by the presence of drag-reducing geometry. The discussion of this effect is deferred until Section 5.

The DNS indicated that in a drag reducing configuration, the significant spanwise variations of the turbulence intensities occur only very near the riblets, while the effect of the "riblets penetrate further into the channel in the drag increasing case" ([8], p. 13 and Fig. 10). The variations of $\partial u/\partial z$ are localized within $y^+ = 10$ for the case $s^+ = 20$, while this region is broader ($y^+ = 30$–40) when the riblets increase the drag. The enhancement of the streamwise vorticity by the twisting term $(\partial v/\partial x)(\partial u/\partial z)$ is therefore localized in a thinner region above the drag reducing riblets. This could lead to a local weakening of the quasi-streamwise vortices. It should be noted however that the contribution of the twisting of ω_z is negligible and the terms in the right hand side of the $D\omega_x/Dt$ equation become of the same order only at the outer edge of the buffer layer ($y^+ > 40$). This reasoning is therefore not convincing.

These arguments provide only a qualitative and global image of the effect of the riblets. They are concentrated on the mechanism within the ribs but they do not clearly explain why the structures are weakened above the drag-reducing riblet wall. It is attempted in the following, to further develop these points of view, by putting the accent on the genesis process.

4. Detailed Analysis of the Regeneration Mechanism – Some Suggestions

The regeneration mechanism as revealed by recent studies presents several subtle details which are not obvious at first glance. To summarize the chain of events during the regeneration processus, we reproduce in Fig. 7 the results obtained by

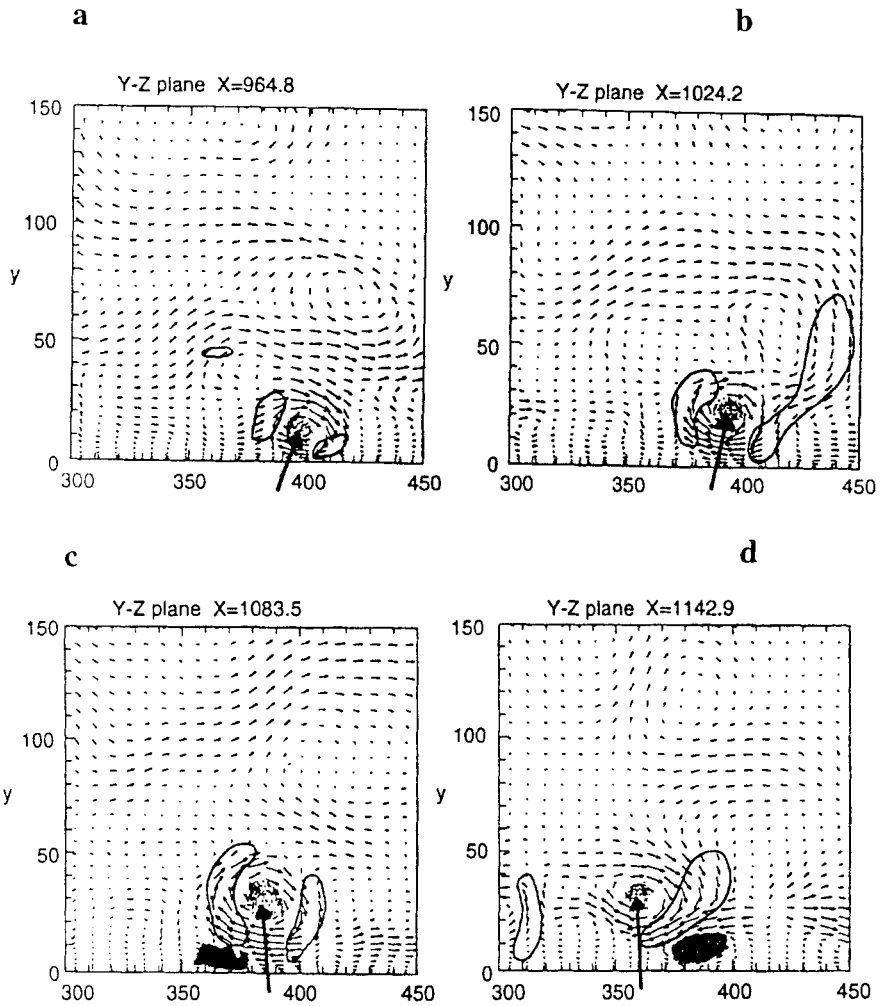

Fig. 7. Evolution of a typical stress-producing eddy in the cross plane at a fixed time reproduced from Brook and Hanratty ([6], Fig. 3 of their paper, p. 1013). The solid encircled areas enclose positive streamwise vorticity regions $\omega_x > 0.2$. The dark areas in Figs c and d correspond to the zones wherein $\omega_x < -0.2$. The mother eddy is shown by arrows.

Brooke and Hanratty ([6], p. 1013). The scenario given by these authors is similar in many aspects to that of Bernard et al. ([5], p. 396).

Figure 7 shows the instantaneous velocity vectors associated with a Reynolds stress producing eddy at a fixed time and different streamwise positions. The mother eddy with $\omega_x > 0$ is shown by arrows. This eddy grows in diameter and the vorticity at its center increases downstream. It is surrounded by two zones of *positive vorticity* in Fig. 7b. The right hand zone almost touches the wall. At the same time, a high pressure zone related to the induced stagnation flow takes place on the right (sweep side of the mother eddy). Further downstream, a *negative*

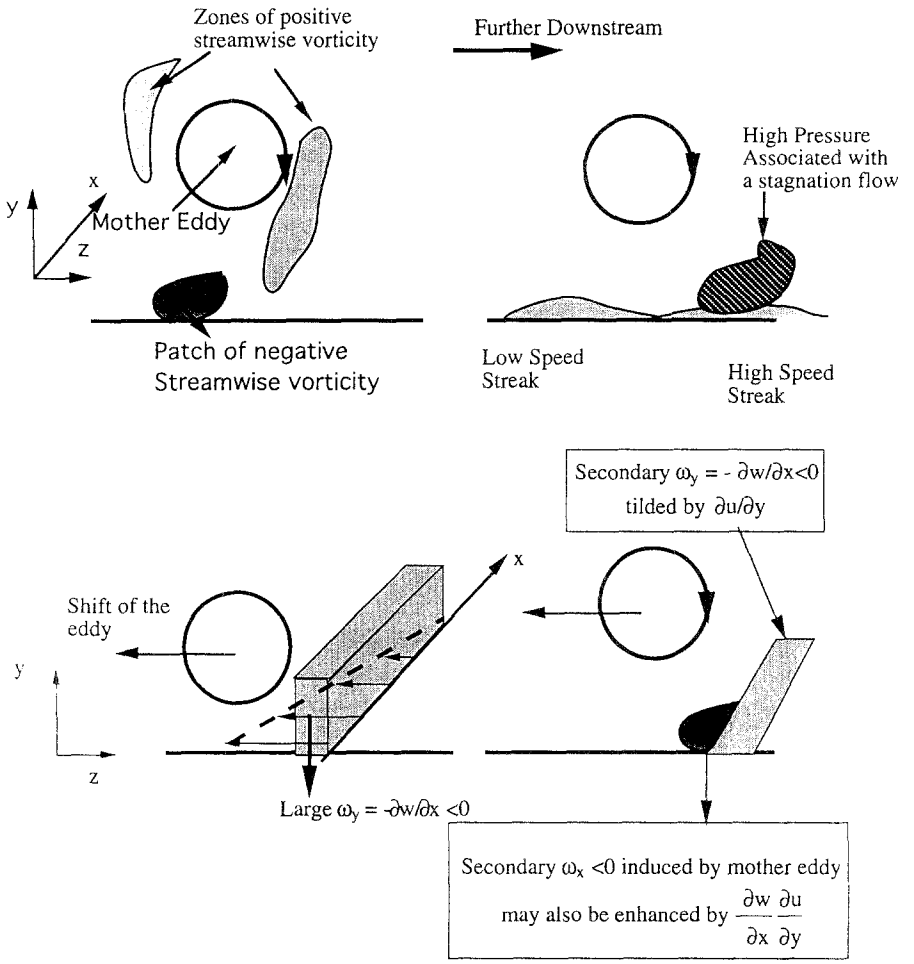

Fig. 8. Structure genesis following Brooke and Hanratty [6] and Bernard et al. [5]. Not on scale.

vorticity zone develops on the left, i.e. the ejection side and diffuses near the wall (Fig. 7c). The final step is the interaction of the high pressure zone associated with the stagnation flow at the sweep side with, presumably, the induced high speed $u' > 0$ streak. The essence of the process is in the creation of a zone where the spanwise velocity is negative (Fig. 8) and progressively increases in magnitude downstream in the negative $-x$ direction. This results in the set up of the streamwise dependence via $\omega_y = -\partial w/\partial x < 0$ which appears as a longitudinal wall vorticity. The high pressure pushes to the left both the mother eddy and the newly created ω_y. This large negative wall normal vorticity is, in return, tilted by the mean shear and enhances the negative vorticity patch through $-(\partial w/\partial x)(\partial u/\partial y)$ (Fig. 8). When the necessary conditions are established, this negative streamwise vorticity

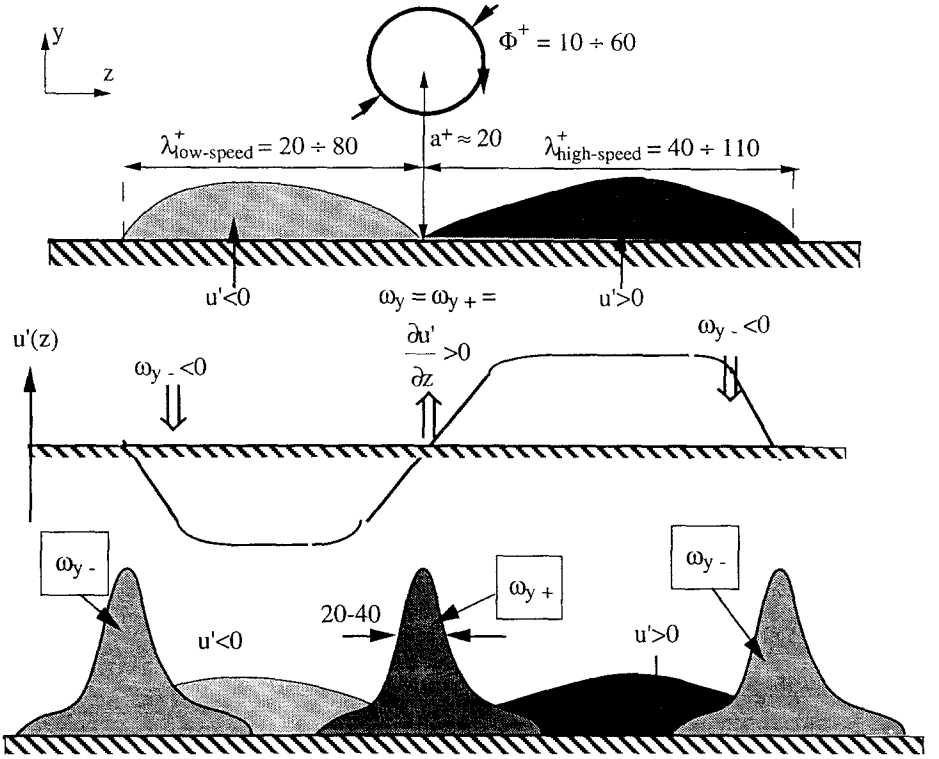

Fig. 9. The streaky structure and sidewalls of wall-normal vorticity associated with a quasi-streamwise vortex. The typical dimensions are given in wall units (not on scale).

may concentrate into a compact core (i.e. roll-up) and regenerates a baby structure opposite to the primary one.

Some of the structural elements commonly observed during the regeneration process shall now be summarized. There is a general consensus on the close relationship between the streaky structure of the near wall turbulence and the presence of the quasi-streamwise vortices in the inner layer. More precisely, the streaks result from the advection of the streamwise momentum by quasi-streamwise vortices advected near the wall with a convection velocity larger than the local one [33]. It is widely accepted that a single quasi-streamwise vortex generates respectively a high speed $u' > 0$ streak at the sweep part of the induced near wall flow and a low speed streak $u' < 0$ at the ejection side with u' being the fluctuating velocity (Fig. 9). The width of the low speed streaks varies between 20–80 wall units. The high speed streaks are wider and their span is between 40–110 according to Robinson [33].

The second structural element is the wall normal vorticity associated with the streaks. One may easily show that near the wall $\omega_y^+ \approx \partial u^+/\partial z^+$. It is therefore expected that the streaks are "surrounded by strong spanwise shear" [37] since they separate alternate zones of high and low streamwise velocity. The wall normal

vorticity near the wall appears essentially as "the sidewalls of the high and low speed streaks" at a certain time and location, as reported by Jiménez and Moin [16]. This is shown schematically in Fig. 9 where layers of positive and negative vorticity are denoted respectively by ω_{y+} and ω_{y-}. The intensity of vorticity in these layers varies between 0.2 and 0.5 wall units. Their spanwise extent is about 20–40 wall units and their streamwise scale is nearly equal to the length of the streaks. Since the former are quite elongated in the streamwise direction, it is logical to assume that $\partial\omega_{y+}/\partial x = \partial\omega_{y-}/\partial x \approx 0$ except of course at the end of the streaks where both vorticity layers terminate. Their y-scale may be quite large with a characteristic thickness decaying towards the tails of their distribution. Later on in this section it is suggested that part of these vorticity layers may play a capital role in the set-up of three-dimensionality during the regeneration cycle.

The third common observation that emerges from both the quasi two-dimensional models [27, 28] and full direct simulations is the formation of layers of secondary x-vorticity of opposite signs at the wall, underneath the parent vortex. Considering that $\partial/\partial x$ is negligible at this initial stage near the primary elongated quasi-streamwise vortex, one has therefore a layer of secondary vorticity $\omega^+_{x,0} = \partial_0 w^+/\partial y^+ < 0$ caused by the mother $\omega^+_x > 0$ eddy. The subindex 0 refers to quantities computed at the wall and $\partial/\partial x$ stands symbolically for the streamwise variation hereafter. There is no clear explanation from past publications concerning the formation of these streamwise vorticity layers. A plausible explanation may be given here if it is recalled that the streamwise vorticity flux at the wall is directly related to the spanwise pressure gradient following $\partial_0\omega^+_x/\partial y^+ = \partial p^+/\partial z^+$. A first order Taylor series gives therefore

$$\omega^+_{x,0} = -\frac{\partial p^+}{\partial z^+}\,\delta y^+ + \omega^+_{x,\delta y^+},$$

where $\omega^+_{x,\delta y^+}$ is the streamwise vorticity at $y^+ = \delta y^+$. A positive spanwise pressure gradient may therefore generate a negative vorticity zone, provided that $\omega^+_{x,\delta y^+} \approx 0$ inside the flow next to the wall, and vice versa. Now, the inviscid flow corresponding to a convecting eddy indicates that the pressure gradient is positive at the left in the ejection zone [12]. More precisely, one may show that the induced pressure gradient in wall units and in a frame of reference moving with the vortex is:

$$\frac{\partial p^+}{\partial z^+} = 2\mathrm{R}^2_{V\mathrm{qs}}\left(1 - \frac{4a^{+2}}{a^{+2}+z^{+2}}\right)\frac{z^+}{(a^{+2}+z^{+2})^2},$$

where $\mathrm{R}_{V\mathrm{qs}} = \Gamma_{\mathrm{qs}}/2\pi\nu$ is the Reynolds number of the (quasi-streamwise) vortex and a^+ is its distance to the wall. This distribution is shown in Fig. 10 for $a^+ = 20$ and $\mathrm{R}_{V\mathrm{qs}} = 22$. It is seen that favorable and adverse pressure gradient zones are respectively located at the sweep and ejection side of the eddy. A model, which is based on an unsteady separation mechanism caused precisely by the local unsteady adverse pressure gradient, is developed by the Lehigh group. This

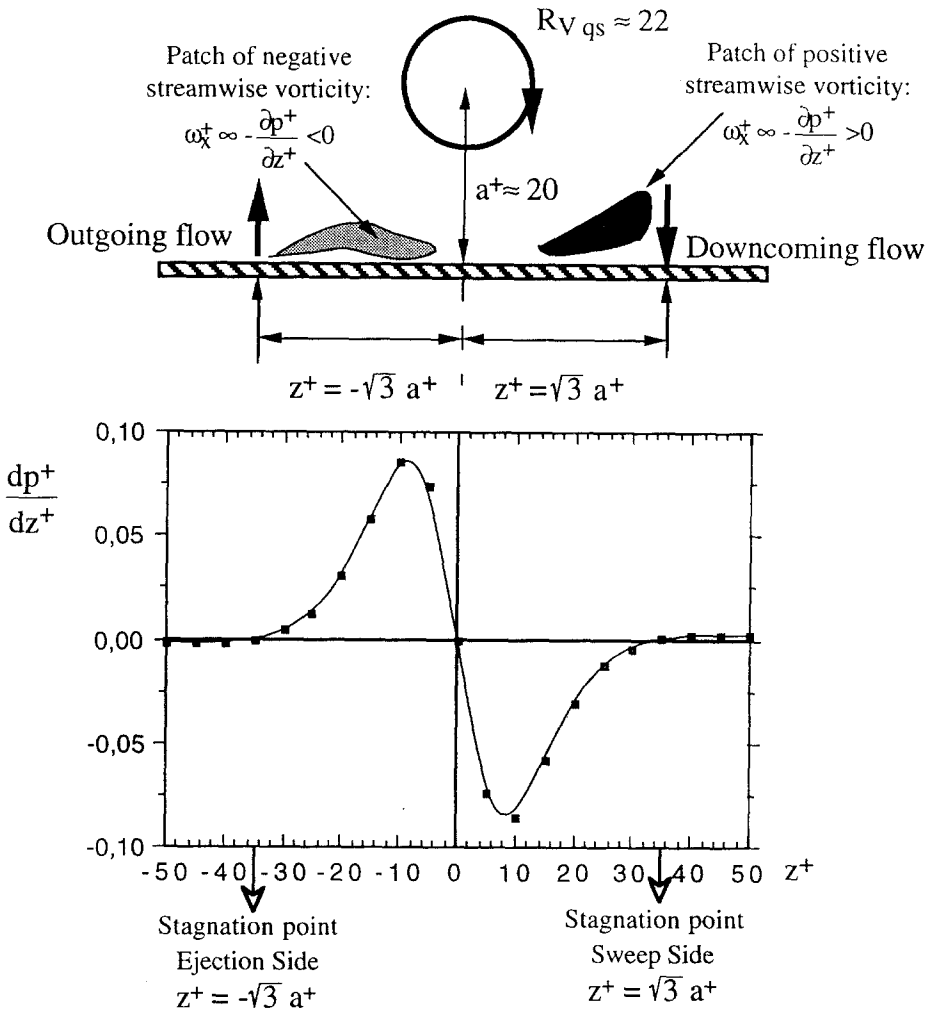

Fig. 10. The pressure gradient in wall units induced by a typical quasi-streamwise vortex. The distance of the point vortex to the wall and its Reynolds number are respectively 20 and 22 wall units. For further details see Smith et al. [36].

mechanism provokes the eruption of new vorticity from the wall by inviscid-viscous interaction. This lift-up, in return, destabilizes the shear layer and generates a secondary structure. The details of this model are nicely summarized in Smith et al. [36] and Walker [47].

Ultimately, two juxtaposed patches of streamwise vorticity are expected near the wall, one being negative and the other positive located respectively at the ejection and sweep sides of the clockwise rotating mother eddy (Fig. 10). This is consistent with the results reported by Brooke and Hanratty (Figs 7b and c). The intensity

and distribution of the vorticity in these layers of course depend on the space-time development of ω_x^+ next to the wall following

$$\omega_{x,0}^+ = -\frac{\partial p^+}{\partial z^+}\,\delta y^+ + \omega_{x,\delta y^+}^+.$$

They are also affected by the development of wall normal velocity associated with the ejection-sweep phenomena through $-\partial v/\partial z_{,\delta y^+}$.

Initially these vorticity patches diffuse. Without any x-dependence they will rapidly dissipate because the enhancement terms in $\boldsymbol{\omega}\cdot\nabla u$ all require a streamwise gradient.

The set-up of the x-dependence and the subsequent enhancement of the negative streamwise vorticity underneath the mother eddy essentially via $-(\partial w/\partial x)(\partial u/\partial y)$ is problematic. The main reason for this complexity is obviously that a streamwise dependence is hardly conceivable in the immediate vicinity of the quite elongated quasi-streamwise vortices. The question that arises is clearly: how is the prevailing x-independent wall normal vorticity transferred to a new wall normal vorticity through $\omega_{y,\text{new}} = -\partial w/\partial x$?

In most of the published studies, the analysis of the regeneration mechanism through the set-up of three-dimensionality is only limited to qualitative descriptions at this stage. We want to go a step further here by suggesting a chain of events which may result in an x-dependent wall normal vorticity. Starting with a $\omega_x^+ > 0$ mother eddy and an immediate near flow with $\partial/\partial x^+ \approx 0$ this task consists in the achievement of $\partial w^+/\partial x^+ > 0$. Subsequently the former is expected to be tilted by the mean shear, at the same time reinforce the negative streamwise vorticity patch and to finally roll-up into a new quasi-streamwise vortex of opposite sign. The necessary conditions for the roll-up are beyond the scope of this paper and some key elements may be found in Jiménez and Orlandi [18].

Let us first determine the vorticity components leading to a streamwise gradient of the spanwise velocity. Given a vorticity field $\boldsymbol{\omega}$, the associated velocity field is:

$$\mathbf{u}(\mathbf{x},t) = -\frac{1}{4\pi}\int \frac{(\mathbf{x}-\mathbf{x}')\wedge\boldsymbol{\omega}(\mathbf{x}',t)}{|\mathbf{x}-\mathbf{x}'|^3}\,\mathrm{d}V(\mathbf{x}').$$

Here, the bold quantities refer to vectors. Suppose that there is a vorticity gradient $\partial\boldsymbol{\omega}(\mathbf{x}')/\partial\mathbf{x}'$ at a given time t, and in some region R. The induced velocity gradient is computed by differentiating the previous relationship and by integrating by parts [17]:

$$\frac{\partial\mathbf{u}}{\partial x_i}(\mathbf{x},t) = -\frac{1}{4\pi}\int_R \frac{(\mathbf{x}-\mathbf{x}')\wedge\frac{\partial\boldsymbol{\omega}(\mathbf{x}',t)}{\partial x_i'}}{|\mathbf{x}-\mathbf{x}'|^3}\,\mathrm{d}V(\mathbf{x}').$$

This gives for the streamwise variation of the spanwise velocity:

$$\frac{\partial w}{\partial x}(x,y,z) = -\frac{1}{4\pi}\int_R \frac{(x-x')\frac{\partial\omega_y}{\partial x'} - (y-y')\frac{\partial\omega_x}{\partial x'}}{[(x-x')^2+(y-y')^2+(z-z')^2]^{3/2}}\,\mathrm{d}x'\,\mathrm{d}y'\,\mathrm{d}z'.$$

It is seen that the streamwise variations of both ω_y and ω_x in a region close to the induced negative x-vorticity may provoke a $\partial w/\partial x$ and a set-up of the three-dimensionality. Both may be a synopsis of the undulatory motion of the low-speed streaks observed by several authors, and, in particular Swearingen et al. [37] during the regeneration of turbulence-production events. Indeed, the wavy motion of the streaks implies both the undulation in x of their sidewalls containing ω_y vorticity and eventually of the quasi-streamwise vortex responsible for the streak formation i.e. the compact ω_x core. Recall, however, that the creation of $\partial w/\partial x$ due to the effect of the stagnation high pressure at the sweep side (Fig. 8) takes place near the wall. This excludes the driving role of $\partial\omega_x/\partial x$ which is expected to be located relatively far from the wall.

It remains to be seen how the variations $\partial\omega_y/\partial x$ give rise to $\partial w/\partial x$. According to Figs 7 and 8 the new $\omega_{y,\text{new}} = -\partial w/\partial x < 0$ builds up somewhere between the sidewalls of $\omega_{y+} > 0$ and $\omega_{y-} < 0$ surrounding the high speed streak. An asymmetrical temporal development of $\partial\omega_y/\partial x$ in the vicinity of this zone may rapidly develop into a bulk of $\omega_{y,\text{new}}$ vorticity as shown conceptually in Fig. 10. Furthermore and according to Brooke and Hanratty (p. 1014) the transfer of existing ω_y to a new $-\partial w/\partial x$ coincides with *the end* of the streaks where both ω_{y+} and ω_{y-} progressively disappear. In the opposite positive x direction one has therefore $\omega_{y+} \propto x^{n+}$ and $\omega_{y-} \propto -x^{n-}$ both exponents being positive. Combining with $\partial\omega_x/\partial x \approx 0$ one has:

$$\frac{\partial w}{\partial x}(x,z,t) \approx \frac{1}{2\pi}\int_R (x-x') \times \left\{ \frac{\frac{\partial\omega_{y+}}{\partial x'}(x',z',t)}{(x-x')^2+(z+z')^2} - \frac{\left|\frac{\partial\omega_{y-}}{\partial x'}(x',z',t)\right|}{(x-x')^2+(z-z')^2} \right\} \mathrm{d}x'\,\mathrm{d}z',$$

where $|\ |$ stands for absolute values. This relationship however is somewhat misleading because the vorticity layers that extend from $x' = \pm\infty$, with a constant gradient of $\partial\omega_{y+(-)}/\partial x'$ (i.e. $\omega_{y+} \propto \omega_{y-} \propto x$) may engender a $w(z)$ but not $\partial w/\partial x$. Indeed, it may be shown by integrating the preceding relationship by parts in x' that:

$$\frac{\partial w}{\partial x} = \frac{1}{4\pi}\int_{-\infty}^{0}\mathrm{d}z'\int_{-\infty}^{+\infty}\frac{\partial^2\omega_{y+}}{\partial x'^2}\log\left[\frac{(x-x')^2+(z+z')^2}{(x-x')^2+(z-z')^2}\right]\mathrm{d}x'$$

$$+\frac{1}{4\pi}\int_{-\infty}^{0}\mathrm{d}z'\int_{-\infty}^{+\infty}\Delta(x',z',t)\log[(x-x')^2+(z-z')^2]\,\mathrm{d}x'$$

for $z < 0$ and an equivalent relationship for $z > 0$. Here

$$\Delta(x',z',t) = \frac{\partial^2\omega_{y+}}{\partial x'^2} - \left|\frac{\partial^2\omega_{y-}}{\partial x'^2}\right|$$

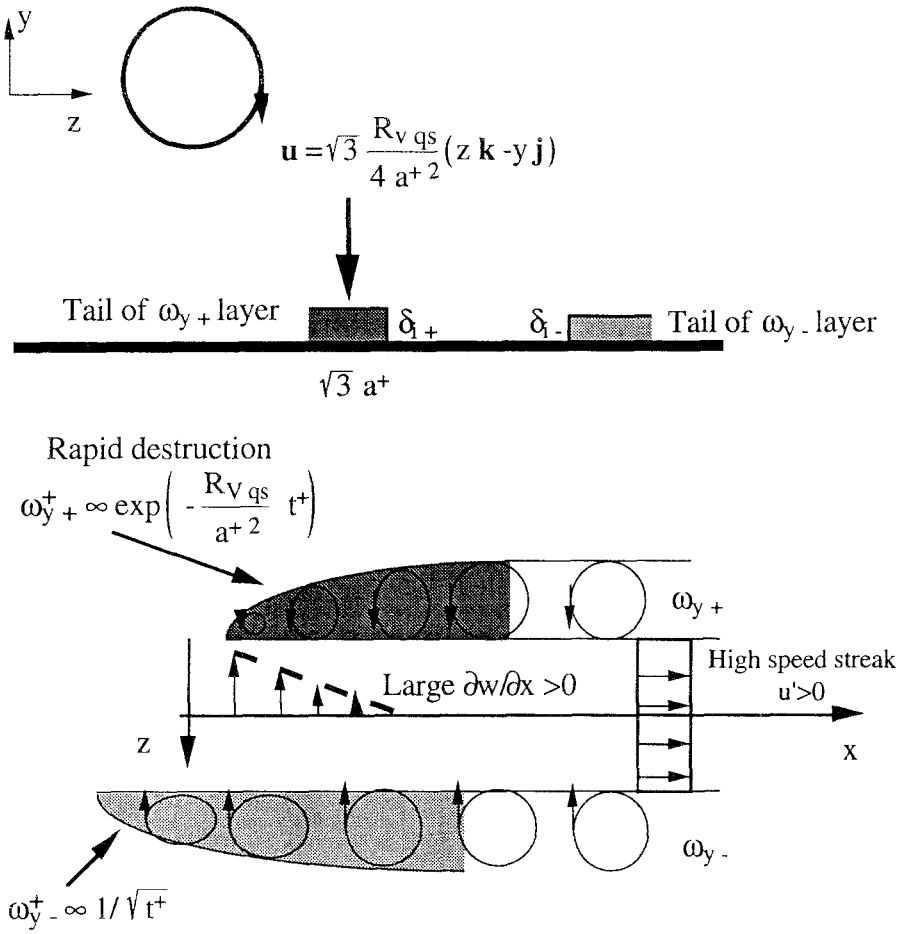

Fig. 11. Conceptual model of x-dependence set-up.

represents the asymmetry between the streamwise evolutions of wall normal vorticity in the positive and negative sidewalls. The first conclusion that may be drawn is that such asymmetry is obviously necessary in order for a local streamwise variation in w to appear near $z \approx 0$. The second conclusion concerns the role of Δ. In the case of $\Delta > 0$, the streamwise gradient of w is unconditionally $\partial w/\partial x > 0$, because both kernels in the integrals are positive. The larger Δ is, the stronger the induced $\omega_{y,\mathrm{new}} = -\partial w/\partial x < 0$ will be. This constitutes the exact condition for the enhancement of the premature $\omega_x < 0$ and the regeneration of a new eddy of opposite sign once of course the conditions for roll-up are fulfilled.

Presumably, when an asymmetry appears in the distribution of the ω_y layers surrounding the flow induced by the mother eddy at the sweep side, a local streamwise variation in w may be introduced and the set-up of the x-dependence starts in the plane (x, z). This may happen for instance when the positive sidewall terminates more rapidly in the $-x$ direction than the negative one or vice-versa (Fig. 11). In

the first case $n_+ \gg n_-$ in the distributions of $\omega_{y+} \propto x^{n+}$ and $\omega_{y-} \propto -x^{n-}$ and consequently $\Delta > 0$. It is logical to assume therefore that a local forcing which quickly razes a part of the ω_{y+} layer induces a new sidewall of $\omega_{y,\text{new}} < 0$ vorticity. The effect of the positive large strain near the stagnation point at the sweep side provides a plausible cause in this process as will now be discussed.

With this aim in mind, consider the evolution of the wall normal vorticity near the quasi-streamwise vortices. Assuming that this evolution is x-dependence free during the early stage of the regeneration process one has:

$$\frac{\partial \omega_y}{\partial t} + v(z,y)\frac{\partial \omega_y}{\partial y} + w(z,y)\frac{\partial \omega_y}{\partial z} = \frac{\partial u}{\partial z}\frac{\partial v}{\partial y} - \frac{\partial u}{\partial y}\frac{\partial v}{\partial z} + \nu \nabla^2 \omega_y.$$

It is seen that without $\partial/\partial x$ the main term $u(\partial \omega_y/\partial x)$ in the redistribution of wall vorticity by advection is missing. On the other hand and since $\partial u/\partial y$ is predominant, the lifting of the spanwise vorticity $(-(\partial u/\partial y)(\partial v/\partial z))$ is expected to overcome the stretching of the normal vorticity $((\partial u/\partial z)(\partial v/\partial y))$ in the source $\boldsymbol{\omega} \cdot \nabla v$. Neglecting the former one has:

$$\frac{\partial \omega_y}{\partial t} + v\frac{\partial \omega_y}{\partial y} + w\frac{\partial \omega_y}{\partial z} = -\frac{\partial u}{\partial y}\frac{\partial v}{\partial z} + \nu\left(\frac{\partial^2 \omega_y}{\partial y^2} + \frac{\partial^2 \omega_y}{\partial z^2}\right).$$

This equation is expected to govern the growth of the wall normal vorticity near the wall and the quasi-streamwise vortices. It manages in particular the sidewalls of ω_y surrounding the streaks shown in Fig. 9.

Next consider, the effect of the mother eddy on such vorticity layers. The pattern vortex structure acts as a single point vortex with a Reynolds number $\mathrm{R}_{V\mathrm{qs}}$, located at $y^+ = a^+$, $z^+ = 0$, in a frame of reference moving with it (Fig. 10). The induced inviscid flow by the vortex and its image have two stagnation points at $z_S^+ = \pm\sqrt{3}\, a^+$ which are located respectively at the sweep and ejection side of the vortex [12]. The induced strain at these points is $\gamma^+ = \pm\sqrt{3}\ (\mathrm{R}_{V\mathrm{qs}}/4a^{+2})$. The typical values of these quantities in a turbulent boundary layer are $z_S^+ = \pm 35$ and $\gamma^+ = \pm 0.02$ obtained with $R_{V\mathrm{qs}} = 22$ and $a^+ = 20$. Figures 9, 10 and 11 show that the stagnation point at the right is located presumably within the ω_{y+} sidewall which has a mean span of about $20 \div 40$ wall units. It is therefore expected that the stagnation flow at the sweep side interacts with the tail of ω_{y+} distribution, where the wall normal scale is smaller than the spanwise one. In this zone the spanwise diffusion of ω_{y+} may therefore be neglected with respect to the wall normal one. Accordingly, the equation governing such ω_{y+}^+ layers near *the stagnation point* is:

$$\frac{\partial \omega_{y+}^+}{\partial t^+} - \gamma^+ y^+ \frac{\partial \omega_{y+}^+}{\partial y^+} = \frac{\partial^2 \omega_{y+}^+}{\partial y^{+2}}\,.$$

This equation describes the development of a Burgers vortex sheet whose asymptotic thickness is determined by the balance between the compression of the vortex

layer and the diffusion. The general similarity solution for a time dependent strain is given by Corcos and Sherman ([10], pp. 61–62). For a constant strain and $y^+ \approx 0$ it takes the form:

$$\omega_{y+}^{+} \propto \frac{\exp(-\gamma^+ t^+)}{\sqrt{\pm \exp(-2\gamma^+ t^+)[\delta_{i+}^{+2} - \delta_a^{+2}] + \delta_a^{+2}}} .$$

In this relationship $\delta_a^+ = \sqrt{\pi/2\gamma^+}$ is the asymptotic thickness of the ω_{y+} layers subjected to the steadily positive strain. The choice of $\pm$ depends on whether the initial thickness δ_{i+} is larger or smaller than δ_a. In the first case the compression will concentrate the vorticity, while, in the second, the thickness of the vorticity layer will increase up to δ_a under the dominating diffusion effect. The asymptotic thickness is reached in a time of about

$$t^+ \approx \left[\left(\frac{2\delta_{i+}^{+2}}{\pi} \gamma^+ \right)^{\pm 1} - 1 \right]^{1/2} \frac{1}{\gamma^+} .$$

For larger times the local vorticity disappears exponentially in time according to $\omega_{y+}^{+} \propto \exp(-\gamma^+ t^+)$. Now, the negative ω_{y-} sidewall is located far away from the stagnation flow. It is primarily under the effect of viscosity. The maximum vorticity in this layer decreases therefore as $\omega_{y-}^{+} \propto 1/\sqrt{t^+}$. Recall also that in a turbulent boundary layer the strain induced by the quasi-streamwise vortices varies between $\gamma^+ = 0.02 \div 0.04$. This implies that for $t^+ \gg 2/\gamma^+$ the positive sidewall disappears almost instantaneously giving rise to a zone of $-(\partial w/\partial x) < 0$. To give a clearer image of this process, suppose that the material points ω_{y+} near the stagnation zone may be viewed as a vortex sheet. Since initially the ω_{y-} layer at the opposite sidewall has approximately the same intensity it may be assigned as the image sheet of ω_{y+}. As much as the strengths $\mathrm{d}\Gamma_+/\mathrm{d}x'$ and $\mathrm{d}\Gamma_-/\mathrm{d}x'$ of these sheets are constants the induced flow is the simple plug potential flow $u' > 0$ corresponding to the high speed streak and the spanwise velocity w is zero. The rapid destruction of the ω_{y+} layer by the stagnation flow is accompanied by a $w < 0$ decreasing in the opposite x-direction in a zone where $\mathrm{d}\Gamma_+/\mathrm{d}x' \propto x'^{n+}$.

This terminates the new suggestion on the regeneration mechanism made in this work and this is summarized in Fig. 12. Note that the approach here is not directly related to a shear layer instability mechanism leading to the streak breakdown discussed in Section 3. Such instabilities may still develop in $\omega_y \propto \partial u/\partial z$ layers under the possible destabilization effect of the terms left out in the vorticity equation. The arguments developed here are not yet based on "clean" computations and should be considered as a first attempt in order to develop a real quantitative theory. There are mainly two points which are encouraging. First of all the generation of new structures is related to the effect of the primary ones by means of an interaction with existing wall normal vorticity layers by a somewhat deterministic scenario. The creation of a new eddy is clearly related to the impingement of sweep flow

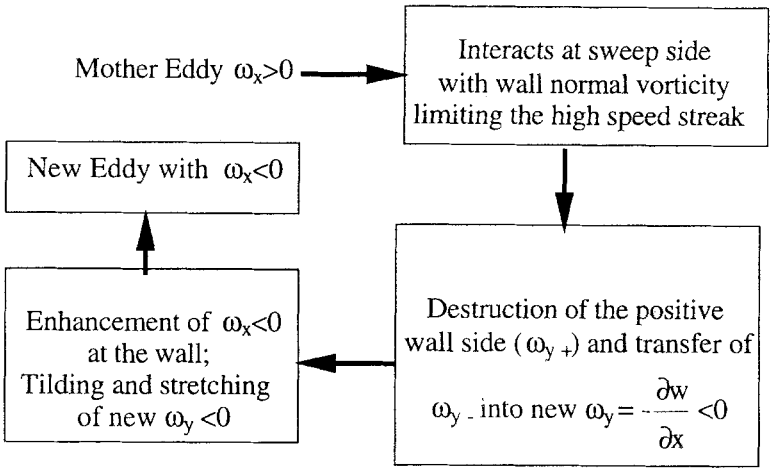

Fig. 12. Conceptual model of the genesis of quasi-streamwise vortices.

caused by the parent structure. The arguments developed here predict correctly the location (in the sweep side underneath the mother eddy) and the rotational sign (opposite to that of the prevailing structure) of the offspring. Secondly the time scale of the regeneration mechanism is related to the structures themselves through $t^+ \propto 2/\gamma^+$ Using the published statistics of the quasi-streamwise vortices one obtains a value of $t^+ = 50 \div 100$ which is curiously close to the ejection period in the buffer layer [24].

According to this point of view, it may be conjectured that the efficiency of the riblets depends upon their capacity to accumulate the wall normal vorticity layers within the ribs and prevent the action of the stagnation flow. Previously, it was pointed out that the spanwise scale of the ω_y layers is about 20 wall units which is close to the ribs spacing in a drag reducing configuration. This effect alone, however would only explain the relative stability of the flow within the ribs or in a region close to, but not the weakening of the structures in the riblets sublayer. This question is analyzed in the next section.

In order that the regeneration cycle be completed one should be sure that the new structure is able to subsequently create x-independent streaks. Hamilton et al. [14] have shown that the source term $-(\partial w/\partial x)(\partial u/\partial y)$ contributes only partially to direct x-independent streamwise vorticity. The x-independent streaks form at later stages of the genesis mainly through the advection $v(\partial\omega_x/\partial y)$. This point is rather new and its role in the control of near wall turbulence is not clear yet.

Finally note that the models based on x-independent Navier–Stokes equation such as investigated by Orlandi and Jiménez [28] are obviously not capable of producing the enhancement mechanism investigated here. Such approaches are quite useful in determining the effect of the longitudinal vortices on the streamwise shear and the roll-up mechanism, as clearly shown by these authors. They indicated for instance that layers of secondary vorticity which are formed at the wall play

an important role in the initial roll-up process but have never been found to roll up into new vortices. This is a natural consequence of the x-independence. What is suggested here is that these secondary vorticity layers may play a more or less significant role in the genesis of the new structures when the three-dimensionality is taken into account.

5. Evolution in Time and Space of the Induced Three-Dimensionality: Effect of the Protrusion Height

The three-dimensional local flow field induced in the vicinity of the quasi-streamwise vortices will develop in time and space further to its set-up. It will dissipate or intensify depending on the nature of its interaction with the base flow. Let the local velocity and vorticity of the former be noted respectively by $\mathbf{U}_i$ and $\boldsymbol{\omega}_i$ where the suffix i stands for the initial flow field generated by quasi-streamwise vortices. The streamwise independence is inherent in $\mathbf{U}_i$ and ω_i with:

$$\boldsymbol{\omega}_i(y,z,t) = \left(\frac{\partial w_i}{\partial y} - \frac{\partial v_i}{\partial z}\right)\mathbf{i} + \frac{\partial u_i}{\partial z}\,\mathbf{j} - \frac{\partial u_i}{\partial y}\,\mathbf{k}.$$

Consider now the evolution of a three-dimensional secondary field superposed to the base flow:

$$\mathbf{U}_s = u_s(x,y,z,t)\mathbf{i} + v_s(x,y,z,t)\mathbf{j} + w_s(x,y,z,t)\mathbf{k}.$$

The corresponding vorticity field is $\boldsymbol{\omega}_s(x,y,z,t)$. The nature of the mechanism which has triggered $\mathbf{U}_s$ does not count: it may, for instance be similar to the one discussed in the previous section, or be due to an instability of some kind coming from the core flow. The objective here is to determine the conditions which make the secondary flow field survive long enough to generate a new structure. In this context and for the reasons discussed before one has to deal essentially with the spatio-temporal evolution of the y-component of the secondary vorticity $\omega_{ys} = \partial u_s/\partial_z - \partial w_s/\partial_x$. This clearly partly corresponds to $\omega_{y\text{new}}$ introduced in the previous section. After splitting, and linearizing around the fields $\mathbf{U}_i$ and $\boldsymbol{\omega}_i$ one obtains:

$$\frac{D\omega_{ys}}{Dt} + \mathbf{U}_s \cdot \nabla\omega_{yi} - \nu\nabla^2\omega_{ys} = \boldsymbol{\omega}_s \cdot \nabla v_i + \boldsymbol{\omega}_i \cdot \nabla v_s,$$

where:

$$\frac{D}{Dt} = \frac{\partial}{\partial t} + \mathbf{U}_i \cdot \nabla.$$

The left hand side regroups the advection of the vorticity by the initial velocity field, its redistribution by the secondary flow and diffusion. Two terms at the right hand side associated respectively *with the initial vorticity field* ($\boldsymbol{\omega}_i \cdot \nabla v_s$) and *the initial flow field* ($\boldsymbol{\omega}_s \cdot \nabla v_i$) make up the enhancement of the secondary normal

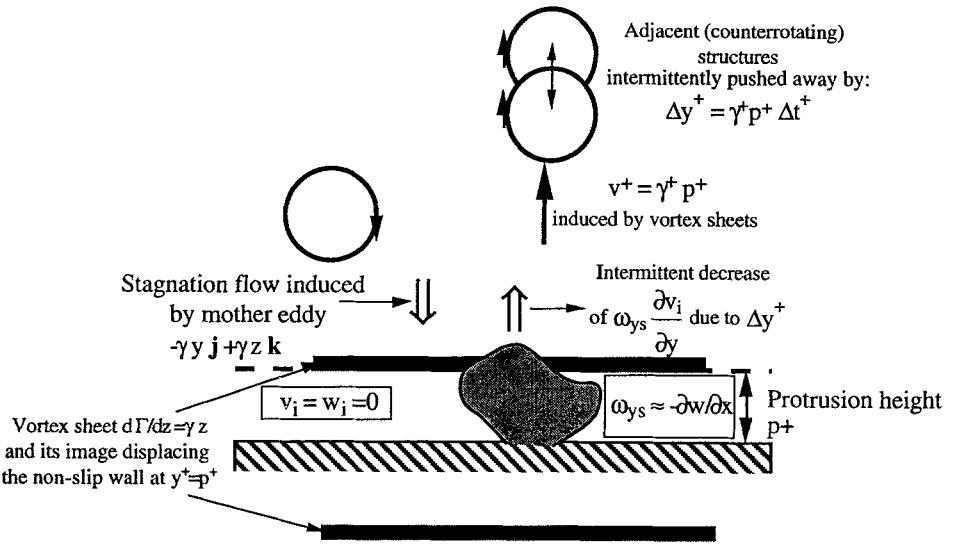

Fig. 13. Intermittent decrease of the enhancement of secondary wall normal vorticity by interaction with protrusion height; see the text (Section 5) for further details (not on scale).

vorticity. The manipulation of the near wall turbulence should consist in controling these couplings which are indirectly but intimately related to the regeneration of new structures through $\omega_{ys}(\partial u/\partial y)$. Preventing these interactions leads to either a decrease of the frequency of active events or/and a reduction of the circulation in the vortices i.e. their Reynolds number. In both cases drag will be reduced.

There are essentially two main enhancement terms in the $D\omega_{ys}/Dt$ equation. The first one is due to the stretching of the initial wall normal vorticity by the secondary v_s gradient through $\omega_{yi}(\partial v_s/\partial y)$. The secondary y-vorticity will also be enhanced when it is stretched by the initial v field i.e. $\omega_{ys}(\partial v_i/\partial y)$ when $\partial v_i/\partial y > 0$. A possibility is the stretching of the newly created vorticity by the outcoming (ejection) stagnation flows induced by adjacent counterrotating eddies (Fig. 13). It is suggested in the following that the main effect of the riblets is to affect directly $\omega_{ys}(\partial v_i/\partial y)$ and reduce indirectly the strength of the offspring.

Let us now concentrate on the effect of the riblets. This task is tremendously facilitated by making use of the well-known protrusion height i.e. the difference between the virtual origins of the viscous longitudinal ($h_=$) and cross flow ($h_\perp$). There is a large consensus by now among the "riblets community" on the fact that the protrusion height $p = h_\perp - h_=$ is a key parameter in the understanding of the drag reduction mechanism [23]. These authors have clearly shown that p is a quantitative characterization of the riblets wall and that the effectiveness of the riblet geometry lies on their capacity of impeding the cross flow more than the longitudinal flow. Consider the "initial" flow field $\mathbf{U}_i$ induced by elongated quasi-streamwise vortices in such a configuration. Since by definition $\partial u_i/\partial x = 0$ the continuity requires that $\partial v_i/\partial y = -\partial w_i/\partial z$ and one has consequently $v_i \approx 0$

in $y < p$ where $w_i \approx 0$ by definition. The riblets geometry in a drag reducing configuration impedes therefore not only the spanwise velocity but also the wall normal velocity as long as the "initial flow field" is considered. The secondary wall normal velocity may of course still penetrate in the zone $y < p$, because in this case $\partial u_s/\partial x \neq 0$. The first conclusion is of course that the enhancement of the "baby" wall normal vorticity through $\omega_{ys}(\partial v_i/\partial y$ is impossible in $y < p$ although the enhancement effect of the secondary field by $\omega_{yi}(\partial v_s/\partial y) = (\partial u_i/\partial z)(\partial v_s/\partial y)$ may still be present. This is the same situation as discussed in Section 2. It leads to the quick dissipation of the structures within the ribs. Secondly, the displacement of the initial flow field in the (y, z) plane may have an indirect consequence on the enhancement of new vorticity by decreasing the stretching as will now be shown.

Imagine the stagnation flow $\gamma z\mathbf{k} - \gamma y\mathbf{j}$ induced by the mother eddy approaching the non-slip wall, now placed at $y^+ = p^+$, because the initial field (v_i, w_i) cannot penetrate deeper (Fig. 13). The non-slip condition requires the subsequent creation of a vortex sheet at $y^+ = p^+$ of strength $\mathrm{d}\Gamma^+/\mathrm{d}z^+ = \gamma z^+$ and an image sheet at $y^+ = -p^+$. It can be shown that these sheets cancel out the potential stagnation flow in $y^+ < p^+$. They induce in return a wall normal velocity $v^+ = \gamma^+ p^+$ [35] which is directly connected to the protrusion height. This positive wall normal velocity pushes away the adjacent quasi-streamwise structures by $\Delta y^+ = v^+ \Delta t^+$ during a time period Δt^+. The former is expected to be short compared with the period of the regeneration process because of the well-known intermittent character of the wall normal velocity [21]. The immediate consequence is the decrease of the strain exerted by the entire initial x-independent flow field at the neighbourhood of the mother eddy. Since $\gamma^+ \propto 1/a^{+2}$ one may estimate this decrease by:

$$\frac{\Delta\gamma^+}{\gamma^+} \approx -2\frac{\Delta y^+}{a^+} \approx -2\frac{\gamma^+ p^+ \Delta t^+}{a^+}.$$

Imagine next that the secondary wall normal vorticity is subsequently provoked. Since the flow is x-dependent by now, one still has $w_s \approx 0$ at $y < p$ but now the continuity requires $\partial v_s/\partial y = -\partial u_s/\partial x \neq 0$ and $v_s \neq 0$ at $y < p$. Therefore, the non-penetration condition for v is shifted down to $y = 0$ i.e. to the $u = 0$ non-slip wall. This requires the creation of fresh vorticity at $y = 0$ which of course does not provoke any additional wall normal velocity. In other words $v^+ = \gamma^+ p^+$ induced previously by the interaction of the initial flow field persists only intermittently and during short time periods. Its main effect is not to affect considerably the position a^+ and/or the radius R^+ of the structures but to reduce their influence on the enhancement of the secondary wall normal vorticity roughly by:

$$\frac{\Delta\omega_{ys} \cdot \nabla v_i}{\omega_{ys} \cdot \nabla v_i} \approx \frac{\Delta\omega_{ys}\frac{\partial v_i}{\partial y}}{\omega_{ys}\frac{\partial v_i}{\partial y}} \approx \frac{\Delta\gamma^+}{\gamma^+} \approx -2\frac{\gamma^+ p^+ \Delta t^+}{a^+}.$$

The weakening of the secondary wall normal vorticity leads to the decrease of the streamwise vorticity by the same amount i.e.

$$\frac{\Delta\omega_x^+}{\omega_x^+} \approx -2\frac{\gamma^+ p^+ \Delta t^+}{a^+},$$

once the regeneration process (including roll-up) is achieved. If it is supposed, that the radius of the vortices is more or less unaffected, the decrease in ω_x^+ results in a decrease of the circulation of the quasi-streamwise vortices through

$$\frac{\Delta\omega_x^+}{\omega_x^+} \propto \frac{\Delta(\Gamma^+/R^{+2})}{\omega_x^+} \propto \frac{\Delta\,\mathrm{R}_{V\mathrm{qs}}}{\mathrm{R}_{V\mathrm{qs}}}.$$

To summarize, the main effect of the riblets is to reduce the strength of the Reynolds shear stress producing eddies by intermittently pushing away the elongated streamwise structures in such a way that the stretching of newly created wall normal vorticity $-(\partial w/\partial x)$ is finally attenuated.

The weaker the quasi-streamwise structures, the smaller the wall shear stress. Indeed, the shear stress at the incoming (sweep) stagnation points is closely related to the total wall shear stress as shown by Orlandi and Jiménez [28]. According to the simplified model reported by these authors, the stagnation flow develops a recirculation bubble of height $2a^+$ and a viscous layer of thickness $\propto \sqrt{1/\gamma^+}$. The maximum shear stress in these layers is

$$\tau^+ = \left(\frac{2}{\pi}\gamma^+\right)^{1/2} u^+(2a^+).$$

Orlandi and Jiménez gives an estimation of the mean wall shear stress by assuming that half of the wall is covered by these high shear layers. This results in

$$\bar{\tau}^+ \approx 0.25\sqrt{\mathrm{R}_{V\mathrm{qs}}}\,\frac{u^+(2a^+)}{a^+}.$$

With $\mathrm{R}_{V\mathrm{qs}}$ between 20–40 and $a^+ = 20$, one obtains $\bar{\tau}^+ \approx 0.7$–1 (instead of one) which is quite satisfactory. This relationship is a rough estimate and should be considered as an indicator of the importance of the quasi-streamwise vortices in the regeneration of the wall shear stress. In reality $\mathrm{R}_{V\mathrm{qs}}$ is Reynolds number dependent, the diameters of the vortices change with y^+, and the mechanism is certainly more complex. Now, if the effect of the riblets is only to weaken the quasi-streamwise vortices by reducing $\mathrm{R}_{V\mathrm{qs}}$ the reduction of drag is simply:

$$\frac{\Delta\bar{\tau}^+}{\bar{\tau}^+} = \frac{\Delta\,\mathrm{R}_{V\mathrm{qs}}}{\mathrm{R}_{V\mathrm{qs}}} \approx -2\frac{\gamma^+ p^+ \Delta t^+}{a^+}.$$

The right hand side of this equation should be interpreted as the additional effect of the riblets with respect to the smooth wall. It is seen that it depends on the short time period Δt^+ during which the vertical "protrusion height-velocity" is active.

It seems to be logical to assume that this time period is of the same order of the duration of Quadrant-2 or Quadrant-4 events, i.e. $\Delta t^+ \approx 20$. Combining this with the typical values of γ^+ and a^+ one finds out that $\Delta\bar{\tau}^+/\bar{\tau}^+ \approx -0.035p^+$ which gives a drag reduction of 3.5 to 7% for $p^+ = 1 \div 2$. These values are close to the results found in the literature.

The mechanism proposed here is the authors personal point of view. It is schematic, partly complete and therefore open to discussion. It is hoped however that it offers some key elements in the understanding of the drag reduction mechanism. The main point is that the riblets intermittently filter the incoming stagnation cross flow by displacing at the same time and during short periods the quasi-streamwise structures and partly prohibiting the enhancement of new structures. The net effect is thought only to be a decrease of R_{Vqs}, without an appreciable change of the standoff distance of the structures nor their size. These points are in agreement with Choi et al. [8]. These authors report a reduction of 12% in the local maximum of the streamwise vorticity fluctuations in a drag reducing case with $s^+ = 20$ and $p^+ \approx 2$. The standoff distance of the quasi-streamwise vortices is not affected by the riblets and "the local maximum (of the vorticity fluctuations) occurs at $y^+ \approx 20$" (with respect to u-non slip wall) regardless of the presence of the riblets which suggests that the center of the streamwise vortex is located on average at $y^+ \approx 20$ as above the smooth wall ([8], p. 15). The diameter of the quasi-streamwise vortices is not affected either which is also in agreement with the model proposed here. If it is supposed therefore that the reduction of R_{Vqs} is roughly equal to the decrease of the local maximum of ω_x one obtains with the preceding relationships a drag reduction of 6% which is exactly the value that Choi et al. [8] obtained. Note finally that this reduction is reasonably well predicted by the estimation $\Delta\bar{\tau}^+/\bar{\tau}^+ \approx -0.035p^+ \approx 0.07$ given before.

There are both concordances and disagreements with the model presented here and the one developed by Jiménez [19]. The model reported by this author starts with an initial perturbation which produces an x-dependence in the streaks. The former are modelled as coflowing jets and the streamwise scale of the perturbation is selected as a multiple of their width. This perturbation is distorted and results in a vertical slab of wall normal vorticity with thickness proportional to λ^+ initially parallel to the cross plane. This may be identified as the secondary x-dependent wall normal vorticity ω_{ys} introduced here. Jiménez argues that the instability causing the x-dependence comes from the core flow and that it is amplified by the natural Kelvin–Helmholtz instability of the thin ω_y layers. This could imply that the time period of the regeneration cycle should be somewhat governed by the outer variables. This is not true for low Reynolds number flows for which it is widely accepted that the bursting frequency scales with inner variables. In the model of Jiménez, the induced x-perturbation is initially fed in the ω_z layer by a perturbation coming from the outer flow and is transferred to ω_{ys} by lifting through $\omega_z(\partial v/\partial z)$. On the contrary, in the model proposed here, ω_{ys} is supplied by a direct effect of the prevailing quasi-streamwise vortices. An attempt is therefore made to relate ω_{ys} to

the cycle of structure genesis but such an effort is not immediately perceptible in the model of Jiménez.

Since there is now an x-dependence, the advection of the secondary vorticity by the mean shear (i.e. tilting) is possible. This is clearly the term

$$\mathbf{U}_i \cdot \nabla \omega_{ysw} \approx u_i(y,z,t)\frac{\partial \omega_{ys}}{\partial x}$$

of the $D\omega_{ys}/Dt$ equation. During this stage the remaining terms of the secondary vorticity equation are left out. At late stages of the tilting, the wall normal vorticity becomes almost parallel to the x-axis and the tilting becomes stretching. The long time limit is therefore a Burger's vortex sheet which is axially strained and diffuses. The short time limit is the advection by the mean shear. When both trends coincide the streamwise vorticity becomes maximum at a given minimum thickness. This thickness stands also for the standoff distance d_s^+ of the quasi-streamwise vortices which result from the roll-up of the vorticity layer. The resulting standoff distance is $d_s^+ \propto \lambda^{+1/3}$. The radius R^+ of the point vortices becomes also a function of λ^+ and is given by $R^+ \propto \lambda^{+2/3}$. The cycle is closed by a feedback equation relating the width of the streaks to R^+ and d_s^+ through $\lambda^+ \propto (R^+ + d_s^+)$. The three equations with unknowns d_s^+, λ^+ and R^+ are combined and good estimates of these quantities are obtained. Finally the circulation Γ^+ in the vortices is also related to the width of the streak assuming that it comes from the one contained in the initial perturbation "which is proportional to the wavelength of the initial instability and therefore to the width of the streak", i.e. $\Gamma^+ \propto \lambda^+$ and the vorticity in the layers should consequently vary like $\omega_x^+ \propto \Gamma^+/R^{+2} \propto 1/\lambda^{+1/3}$. The main conclusion is that the key parameters are on the whole related to the standoff distance of the layers of streamwise vorticity. The control of wall friction is therefore equivalent to the control of d_s^+. Large d_s^+ results in drag reduction, i.e. the drift of the streamwise vorticity layers decreases the wall shear stress. According to Jiménez [19] the riblets imposes such a permanent drift in a drag-reducing configuration. This drift acts intermittently in the model proposed here.

6. Forcing Control Experiments and Their Consequences on the Spatio-Temporal Development of the Wall Shear-Stress

The recent investigation of Jiménez [19] will now be discussed. This author relates the effect of the riblets to a shift of the standoff distance of the streamwise vorticity layers. His suggestion is motivated by the results of a numerical control experiment. He introduces the protrusion height p in an intrinsic way, by intervening in the transverse non-slip condition through continuous forcing of the spanwise velocity at the (u,v) non-slip wall. He fixes the spanwise velocity as $w(x^+,0,z^+,t^+) \approx -\alpha w(x^+,y^+=10,z^+,t^+)$. Such a forced intervention in the boundary conditions at the wall results in a drift of the location of the maximum of the transverse turbulence intensity by $p^+$when $\alpha > 0$. Jiménez argues that this translation may

be a consequence of the drift Δd_s^+ of the standoff distance streamwise vorticity layers away from the wall. A closer look at his data reveals that $p^+ \approx 4\alpha$ in the range $p^+ = 1 \div 2$. By assuming that w varies linearly in y near the wall, one may show that the forcing:

$$w(x^+, 0, z^+, t^+) \approx -\alpha w(x^+, y^+ = 10, z^+, t^+)$$

becomes equivalent to $w(x^+, 0, z^+, t^+) \approx -w(x^+, 2p^+, z^+, t^+)$ which in turn, places instantaneously the virtual transverse wall at $y^+ \approx p^+$. The drift Δd_s^+ results in:

- an increase in the streak spacing, by: $\Delta\lambda^+/\lambda^+ \approx 3(\Delta d_s^+/d_s^+)$;
- thickening of the vortices by: $\Delta R^+/R^+ \approx 2(\Delta d_s^+/d_s^+)$;
- an increase in the circulation: $\Delta\Gamma^+/\Gamma^+ \approx 3(\Delta d_s^+/d_s^+)$;
- a decrease in the streamwise vorticity by: $\Delta\omega_x^+/\omega_x^+ \approx -(\Delta d_s^+/d_s^+)$;

and a decrease in the wall shear stress by:

$$\frac{\Delta\bar{\tau}^+}{\bar{\tau}^+} \approx \frac{1}{2}\frac{\Delta\Gamma^+}{\Gamma^+} - \frac{\Delta a^+}{a^+} = -2\frac{\Delta d_s^+}{d_s^+}\,.$$

Finally the standoff distance is related to p^+ by $\Delta d_s^+/d_s^+ \approx 0.04p^+$. It is seen that these estimations give a drag reduction of 8 to 16% for $p^+ = 1 \div 2$ which seems to be overestimated. On the other hand, the decrease in the wall shear stress should be twice as great as the decrease in the streamwise vorticity while the inverse is reported by Choi et al. [8] as discussed in the previous section. Furthermore, an increase of 8–16% of the diameters of the quasi-streamwise vortices predicted by the model is not confirmed by the DNS results of Choi either. More data is undoubtedly necessary in particular that dealing with the statistics corresponding to the vortices in the riblets layer before drawing a firm conclusion.

It would be instructive at this stage to state the consequences of a forced non-slip condition $w(x, y = 0, z, t) \neq 0$ on the vorticity dynamics. Consider first the evolution equation of the spanwise vorticity $\omega_{z,0} = -\tau$ at the (u, v) non-slip wall:

$$\frac{\partial\omega_{z,0}}{\partial t} + w_0\frac{\partial_0\omega_z}{\partial z} = \omega_{x,0}\frac{\partial_0 w}{\partial x} + \omega_{y,0}\frac{\partial_0 w}{\partial y} + \omega_{z,0}\frac{\partial_0 w}{\partial z} + \nu\nabla_0^2\omega_z.$$

Recall that the subindex 0 refers to quantities computed at the wall. We have therefore:

$$\begin{aligned}\frac{\partial\omega_{z,0}}{\partial t} + w_0\frac{\partial_0\omega_z}{\partial z} &= -\frac{\partial_0 v}{\partial z}\frac{\partial_0 w}{\partial x} + \frac{\partial_0 u}{\partial z}\frac{\partial_0 w}{\partial y} + \left(\frac{\partial_0 v}{\partial x} - \frac{\partial_0 u}{\partial y}\right)\frac{\partial_0 w}{\partial z} + \nu\nabla_0^2\omega_z \\ &= -\frac{\partial_0 u}{\partial y}\frac{\partial_0 w}{\partial z} + \nu\nabla_0^2\omega_z.\end{aligned}$$

The difference of this equation with respect to the conventional $w = 0$ non-slip transverse flow configuration is in the presence of the advection term at the

left hand side and the enhancement term at the right. Spanwise averaging $\langle\ \rangle$, with $\langle \partial/\partial z \rangle = 0$ leads to the same result reported by Orlandi and Jiménez [28] namely:

$$\frac{\partial \langle \omega_z, 0 \rangle}{\partial t} = 2 \left\langle \omega_{z,0} \frac{\partial_0 w}{\partial z} \right\rangle + \nu \left\langle \frac{\partial_0^2 \omega_z}{\partial y^2} \right\rangle .$$

The non-linear source term at the right comes from the stretching *and* the spanwise advection of the spanwise vorticity at the wall which becomes equal in magnitude when the averaging is processed. Now, the forcing $w(x, 0, z, t) = -w(x, 2p, z, t)$ implies roughly that:

$$\frac{\partial_0 w}{\partial y} \approx \frac{\partial_{2p} w}{\partial y}$$

but

$$\frac{\partial_0 w}{\partial x} \approx -\frac{\partial_{2p} w}{\partial x} \quad \text{and} \quad \frac{\partial_0 w}{\partial z} \approx -\frac{\partial_{2p} w}{\partial z} .$$

The subindices in these relationships refer as usual, to the y positions where the quantities are performed. Furthermore, in the x-independent flow near the quasi-streamwise vortices, $\partial_0 v/\partial y \approx -(\partial_{2p} v/\partial y))$ by continuity. In these circumstances, the source term in the $\omega_{z,0}$ equation becomes $2\langle \omega_{z,0}(\partial_{2p} v/\partial y)\rangle$. This implies, for instance that a local zone of *high* spanwise vorticity at $y = 0$, is enhanced by an outcoming flow which develops *above* the transverse wall. The conditions for the generation of spanwise vorticity at $y > p$ are, however opposite to those at the u–v non-slip wall. Consider indeed the evolution of $\langle \omega_{z,p} \rangle$ at $y = p$. Since $\partial_p v/\partial y \approx 0$ when $\partial/\partial x \approx 0$, the wall normal velocity near $y = p$ is mainly governed by $\partial_p^2/\partial y^2$ and

$$v \approx \frac{1}{2}[(y-p)^2 - p^2] \frac{\partial_p^2 v}{\partial y^2}$$

provided that p is small. It may be shown, in these conditions that $\langle \omega_{z,p} \rangle$ is given by:

$$\begin{aligned} \frac{\partial \langle \omega_{z,p} \rangle}{\partial t} &= -\left\langle \frac{\partial_p}{\partial y} (v\omega_z) \right\rangle + \left\langle u_p \frac{\partial_p^2 v}{\partial y^2} \right\rangle + \nu \nabla^2 \langle \omega_{z,p} \rangle \\ &\approx -\left\langle \frac{\partial_p}{\partial y} (v\omega_z) \right\rangle - \frac{2}{p} \langle v_p \omega_{z,p} \rangle + \nu \nabla^2 \langle \omega_{z,p} \rangle . \end{aligned}$$

The last relationship was obtained by using

$$v_p \approx -\frac{1}{2} \frac{\partial_p^2 v}{\partial y^2} p^2 \quad \text{and} \quad u_p \approx -\omega_{z,p} p .$$

It is clearly seen that an outcoming flow $v_p > 0$ above the transverse wall enhances a *low* spanwise vorticity zone and not a high one. In other words, the forcing impedes and constrains to $y < p$ the expansion of the spanwise vorticity fluctuations each time, a low or high shear stress zone is reinforced at $y = 0$. During such time periods, the wall shear stress is generated in a more localized fashion compared with the standard boundary layer. If it is supposed that a similar mechanism takes place near the riblets, this argument may explain why the effect of the surface change is localized within a narrow region when there is decrease of drag [8]. This does not provide a clear explanation of the drag reduction in the forced conditions for all that.

The second and the third differences inferred by the artificial forcing are in the modifications of the spanwise averaged streamwise and wall normal vorticities at $y = 0$:

$$\frac{\partial\langle\omega_{x,0}\rangle}{\partial t} = \left\langle -\frac{\partial_0 w}{\partial x}\frac{\partial_0 u}{\partial y}\right\rangle + \left\langle \omega_{x,0}\frac{\partial_0 w}{\partial z}\right\rangle + \nu\langle\nabla_0^2\omega_x\rangle$$

$$\frac{\partial\langle\omega_{y,0}\rangle}{\partial t} = \nu\langle\nabla_0^2\omega_y\rangle.$$

It has to be noted that $\langle\omega_{y,0}\rangle = -\langle\partial_0 w/\partial x\rangle = 0$ for a non-slip wall on which the streamwise vorticity may only diffuse. This also implies that the vorticity flux at the virtual wall is not necessarily instantaneously balanced by the pressure gradient i.e. $\partial p^+/\partial z^+ \neq \partial\omega_x^+/\partial y^+$ [22]. According to $\partial_0 w/\partial x \approx -(\partial_{2p} w/\partial x$ it may be clearly conjectured that once an x-dependent wall normal vorticity $\omega_{y,\text{new}} \approx -(\partial w/\partial x)_{y>2p}$ is established somewhere above the $w = 0$ wall at $y = p$, a part of this vorticity is transferred to $y = 0$ but with opposite sign i.e. $\omega_{y,0,\text{new}} \propto -\omega_{y,\text{new}_{y>2p}}$ (with of course the corresponding image vorticity layers). The wall normal vorticity $\omega_{y,\text{new}_{y>2p}}$ eventually enhances a streamwise vorticity layer as discussed before but now, an equivalent less intense $\omega_{x,0} \propto -\omega_{x,0_{y>2p}}$ layer with opposite sign near $0 < y < p$ is generated too. It may be speculated that the subsequent advection of this opposite vorticity into $y > p$ will weaken the quasi-streamwise vortices during the growth-up. The opposite thin vorticity layers at $y < p$ hardly role up into secondary quasi-streamwise vortices which could affect the wall shear stress. The drag is therefore almost solely governed by the weakened quasi-streamwise structures located at $y > p$ and is consequently reduced. Even in the case where there is roll-up, the effect of the secondary quasi-streamwise vortices on the local shear would be opposite through the stretching $-\tau(\partial_0 v/\partial y)$: when the structure at $y > p$ enhances the wall shear stress at the incoming stagnation point, the secondary structure beneath would act oppose it by compressing the spanwise vorticity layer. The indirect consequence of this process is the set-up of a $\overline{w^2}$ profile in $y < p$ with a maximum at $y = 0$ due to the diffusion of the induced opposite streamwise vorticity, and a decrease in the local maximum of the $\overline{w^2}$ profile at $y > p$ due to the same effect. This is along the same lines as the results reported by Jiménez ([19], Fig. 3). The thickness of the $\overline{w^2}$ profile defined

as the distance between the local minimum at $y = p$ and the maximum above is not affected as expected. In other words, the location of the quasi-streamwise vortices above $y = p$ is equal to that of the structures above a smooth wall. This interpretation is different from the one given by Jiménez [19], in that the drift of the standoff distance of streamwise vortices does not intervene here.

It is highly questionable to argue that such artificial boundary conditions may model the structure of the flow in the presence of the riblets. The intermittent model proposed in the previous section only makes use of the differences in the virtual origins without a selective interference with the existing sublayer turbulence. The personal view of the author is that the passive drag-reduction mechanism driven by the riblets have different facets compared with the artificial introduction of spanwise velocity at the wall.

7. "Filtering" Effect of the Riblets

We will end here by making a final comment on the spanwise correlations of the streamwise velocity near the riblets performed by Chu and Karniadakis ([9], Fig. 13). Their results are reproduced in Fig. 14a. The spanwise correlations of the streamwise velocity $R_{u'u'}(z^+)$ are computed by these authors at respectively $y^+ \approx 32$ above the smooth wall and $y^+ \approx 24$ above the riblet tips. It is clearly seen in Fig. 14a that the minimum in $R_{u'u'}(z^+)$ in the riblets sublayer is much more pronounced compared with the smooth wall. This minimum is related to streak spacing. Naguib and Wark [26] have shown that the negative correlation peak in the spanwise correlation curve $R_{\tau'u'}$ of wall shear stress and the streamwise velocity fluctuations in the standard buffer layer exists only within certain frequency bands. More clearly, the near wall eddies which correspond to high frequency structures (obtained by high pass filtering of the signals with a cut-off frequency of typically $f^+ = 0.0025$) are responsible for the negative deep. The contribution of the outer low-frequency structures to $R_{\tau'u'}$ weakens and even suppresses the local minimum. We have recently repeated these measurements in a channel flow at $y^+ = 12$ and we show the results in Fig. 14b to fix the ideas [44]. The spanwise correlations of the streamwise velocity in the low buffer layer are qualitatively similar to $R_{\tau'u'}$. Now, the fact that the negative correlation peak in $R_{u'u'}(z^+)$ above the riblets is quite pronounced, could indicate that the "noisy" effect of the outer structures is of minor importance. This, in return, implies that the riblets filter the outer structures and that the "inactive" motions penetrate the riblets wall region less.

8. Conclusion

The effect of the riblets on drag producing vortical structures is analyzed by means of near wall vorticity dynamics. The attention is first focused on the flow within and immediately above the ribs. It is conjectured that the riblets shorten the time period necessary for the spatio temporal development of the low speed streak instability

a

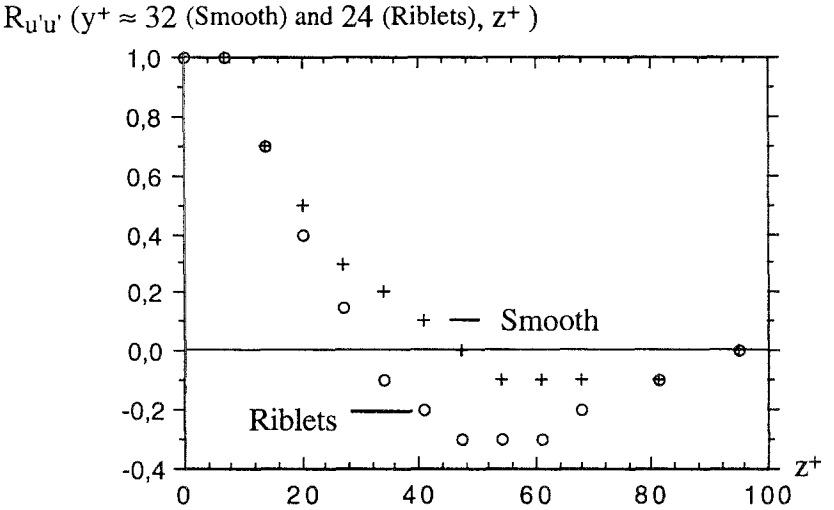

b

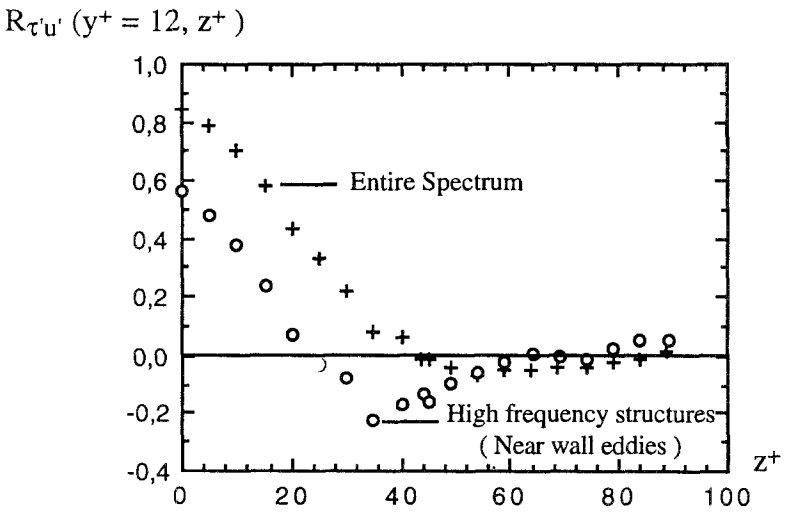

Fig. 14. (a) Spanwise correlation of the fluctuating streamwise velocity according to Chu and Karniadakis [9]. Re = 3500 (based on centerline velocity). The y^+ locations are shown on the figure. (b) Spanwise correlation of the fluctuating wall shear stress and the streamwise velocity in a standard boundary layer at $y^+ = 12$ according to Vezin et al. [44]. Is also shown the correlation curve of high pass filtered signals corresponding to the active eddies [26]. Re = 8000.

in drag reducing configurations. The break-up of the spanwise vortex filaments is inhibited, and only those spanwise vortical structures with low Reynolds numbers are subjected to long-wavelength instability resulting in small growth rates. Since, DNS indicated that significant spanwise variations occur very near the riblets when they decrease the drag, it is also suggested that the enhancement of the streamwise vorticity through the twisting term $(\partial v/\partial x)(\partial u/\partial z)$ should be localized in a thinner region, compared with the drag increasing riblets.

The main enhancement term in the streamwise vorticity generation equation is the tilting of the wall normal vorticity through $-(\partial w/\partial x)(\partial u/\partial y)$. The genesis of new quasi-streamwise vortices depends upon the capability of the primary structures to regenerate x-dependent intense wall normal vorticity $-(\partial w/\partial x)$. This is somewhat problematic, because a streamwise dependence is hardly conceivable in the immediate vicinity of elongated streamwise structures. An extensive analysis combined with some recent observations inferred from DNS suggested a chain of events which leads to a secondary x-dependent wall normal vorticity. It is shown that the impingement of sweep flow caused by a parent structure razes rapidly one of the sidewalls of the (initially x-independent) high speed streak. This leads to a local asymmetry between the streamwise evolutions of wall normal vorticity in the positive and negative sidewalls, resulting in a secondary $-(\partial w/\partial x)$. The former is tilted by the shear and regenerates a new quasi-streamwise structure opposite to the prevailing one. The predicted time scale of the regeneration processus is close to the ejection period in the buffer layer.

The space-time evolution of this secondary x-dependent field reveals that it is partly enhanced through the stretching of the newly created sidewall vorticity by the existing primary wall normal velocity field. In the presence of the riblets, and near the elongated flow structures the primary flow is x-independent and the cross flow can not penetrate into the protrusion height p. The non-slip condition requires the creation of a vortex sheet and its associated image at $y = \pm p$. These vortex sheets cancel out the flow generated by a primary structure in $y < p$. They induce, in return, an intermittent positive wall normal velocity which pushes away the adjacent quasi-streamwise structures. This results in a decrease of the strain they exert on the near wall flow at their ejection side, because the strain is inversely proportional to the square of their distance to the wall. The direct consequence is the reduction of the enhancement of secondary wall normal vorticity through stretching. The indirect consequence is the weakening of the quasi-streamwise vorticity layers and of the quasi-streamwise vortices after the roll-up. Since the wall shear stress is related to the Reynolds number of these structures, a decrease of $\bar{\tau}$ is obtained. The model gives reasonable estimations of the amount of drag reduction.

The last part of this paper is devoted to the discussion concerning the differences between the model presented in this study and that inferred from forcing control experiments. In these experiments, the spanwise velocity at the (u, v) non-slip wall is artificially introduced out of phase with the w velocity detected in the buffer

layer. The consequences of forced non-slip condition on the vorticity dynamics are analyzed with a double aim, first in order to understand why the drag is reduced in such experiments, and second to determine how this forcing affects the near wall vorticity dynamics. The analysis of the spanwise vorticity equation reveals that the forcing constrains the generation of the spanwise vorticity fluctuations into a thin zone, each time a low or high shear stress zone is reinforced at the wall. It is conjectured that this may explain why, the effect of the riblets is localized within a narrow region in drag decreasing configurations. The artificial forcing changes the structure of the streamwise vorticity equation in such a way that, the quasi-streamwise structures above the transverse $w = 0$ wall are weakened because of the effect of the streamwise vorticity layers of opposite sign generated by the forcing below. These mechanisms differ from those governed by the intermittent model proposed here.

As one of the referees has pointed out, the analysis presented in this paper is based on the indirect assumption that $\partial w/\partial x$ has a "time dependent coherent" part. Although, a number of recent studies indicate that this is indeed the case, further investigations are still needed in order to clarify the genesis process of the turbulence producing eddies.

Acknowledgements

The author is grateful to Miss Carmel McDermott for her patience and her support during the accomplishment of this work. Thanks are also due to the referees for their advices and comments.

References

1. Bacher E.V. and Smith, C.R., A combined visualization-anemometry study of the turbulent drag reducing mechanism of triangular micro-grove surface modifications. AIAA paper AIAA–85–0548 (1985).
2. Bechert, D.W. and Bartenwerfer, M., The viscous flow on surfaces with longitudinal ribs. *J. Fluid Mech.* 206 (1989) 105.
3. Bechert, D.W., Bartenwerfer, M. and Hoppe, G., Turbulent drag reduction by nonplanar surfaces – A survey on the research at TU/DLR Berlin. In: Gyr, A. (ed.), *Proc. IUTAM Symp. Structure of Turbulence and Drag Reduction*, Zurich, 25–28 July 1989. Berlin: Springer-Verlag (1990) pp. 525–543.
4. Benhalilou, M., Anselmet, F. and Fulachier L., Conditional Reynolds stress on a V-grooved surface. *Phys. Fluids* 6(6) (1994) 2101.
5. Bernard, P.-S., Thomas, J.-M. and Handler, R.-A., Vortex dynamics and the production of Reynolds stress. *J. Fluid Mech.* 253 (1993) 385.
6. Brooke, J.-W. and Hanratty, T.J., Origin of turbulence-producing eddies in a channel flow. *Phys. Fluids* A5(4) (1993) 1011.
7. Choi, K.-S., Near-wall structure of a turbulent boundary layer with riblets. *J. Fluid Mech.* 298 (1989) 417.
8. Choi, H., Moin, P. and Kim, J., Direct numerical simulation of turbulent flow over riblets. CTR Manuscript, Stanford University, Stanford, CA 94305–3030 (1992); also, *J. Fluid Mech.* 255 (1993) 503.

9. Chu, D.C. and Karniadakis, G.E., A direct numerical simulation of laminar and turbulent flow over riblet mounted surfaces. *J. Fluid Mech.* 250 (1993) 1.
10. Corcos, G.M. and Shermann, F.S., The mixing layer: Deterministic models of a turbulent flow. Part 1: Introduction and the two-dimensional flow. *J. Fluid Mech.* 139 (1984) 29.
11. Corcos, G.M. and Lin, S.J., The mixing layer: Deterministic models of a turbulent flow. Part 2: The origin of the three dimensional motion. *J. Fluid Mech.* 139 (1984) 67.
12. Doligalski, T.-L. and Walker, J.D.-A., The boundary layer induced by a convected two-dimensional vortex. *J. Fluid Mech.* 139 (1984) 1.
13. Gallagher, J.A. and Thomas, S.W., Turbulent boundary layer characteristics over streamwise grooves. AIAA Paper 84-2185 (1984).
14. Hamilton, J.M, Kim, J. and Waleffe, F., Regeneration of near-wall turbulence structures. In: *Ninth Symp. on Turbulent Shear Flows*, Kyoto, Japan, August 16–18 (1993) pp. 11-5-1/11-5-6.
15. Hooshmand, D., Youngs, R. and Wallace, J.M., An experimental study of changes in the structure of a turbulent boundary layer due to surface geometry changes. AIAA paper AIAA–83–0230 (1983).
16. Jiménez, J. and Moin, K., The minimal flow unit in near wall turbulence. *J. Fluid Mech.* 225 (1991) 213.
17. Jiménez, J., Kinematic alignment effects in turbulent flows. *Phys. Fluids* A4(4) (1992) 652.
18. Jiménez, J. and Orlandi, P., The rollup of a vortex layer near a wall. *J. Fluid Mech.* 248 (1993) 297.
19. Jiménez, J., On the structure and control of near wall turbulence. *Phys. Fluids* 6(2) (1994) 944.
20. Kawahara, G., Ayukawa, K. and Ochi, J., On the origin of streaky structures in wall-bounded turbulent flows. In: So, R.M.C, Speziale, C.G. and Launder, B.E. (eds), *Near Wall Turbulent Flows*. Amsterdam: Elsevier (1993) pp. 403–412.
21. Landahl, M.T., On sublayer streaks. *J. Fluid Mech.* 212 (1990) 593.
22. Lightill, M.J., In: Rosenhead, L. (ed.), *Boundary Layer Theory in Laminar Boundary Layers*. Oxford: Oxford University Press (1963) Ch. 11.
23. Luchini, P., Manzo, F. and Pozzi, A., Resistance of a grooved surface to parallel and cross-flow. *J. Fluid Mech.* 228 (1991) 87.
24. Luchik, T.S. and Tiederman, W.G., Timescale and structure of ejections and bursts in turbulent channel flows. *J. Fluid Mech.* 174 (1987) 529.
25. Lumley, J.L. and Kubo, I., Turbulent drag reduction by polymer additives: A survey. Sibley School of Mech. and Aero. Eng., Rep. FDA-84-07, Cornell University, Ithaca, NY (1984).
26. Naguib, A.M. and Wark, C.E., An investigation of wall-layer dynamics using a combined temporal filtering and correlation technique. *J. Fluid Mech.* 243 (1992) 541.
27. Orlandi, P. and Jiménez, J., A model for bursting of near wall vortical structures in boundary layers. In: *Eight Symposium on Turbulent Shear Flows*, Technical University of Munich, September 9–11. (1991) pp. 28-1-1/28-1-6.
28. Orlandi P. and Jiménez, J., On the generation of turbulent wall friction. *Phys. Fluids* 6(2) (1994) 634.
29. Phillips, W.R.C., Coherent structures and the generalized Lagrangian mean equation. *Appl. Mech. Rev.* 43(5) (1990) S227.
30. Phillips, W.R.C., On the etiology of shear layer vortices. *Theor. Comput. Fluid Dynamics* 2 (1991) 329.
31. Phillips, W.R.C, The genesis of streamwise vortices in a turbulent wall layer. In: Bonnet, J.P. and Glauser, M.N. (eds), *Proc. of Iutam Symp. on Eddy Structure Identification in Free Turbulent Shear Flows*. Dordrecht: Kluwer Academic Publishers (1993) pp. 35–41.
32. Robinson, S.K., Kline, S.J. and Spalart, P.R., Quasi-coherent structures in the turbulent boundary layer: Part II. Verification and new information from a numerically simulated flat plate layer. In: *Zoran P. Zarić Memorial International Seminar on Near-Wall Turbulence*, 16–20 May 1988, Dubrovnik, Yugoslavia (1988) pp. 3.1–3.38.
33. Robinson, S.K., The kinematics of turbulent boundary layer structure. NASA Technical Memorandum 103859 (1991).

34. Sendstad, O. and Moin, P., The near wall mechanics of three-dimensional turbulent boundary layers. Thermosciences Div. Rep. TF-57. Stanford University, Department of Mechanical Engineering (1992).
35. Sherman, F.-S., *Viscous Flow*. New York: McGraw-Hill (1990).
36. Smith, C.R., Walker, J.D.A, Haidari, A.H. and Sobrun, U., On the dynamics of near wall turbulence. *Philos. Trans. R. Soc. London Ser.* A336 (1991) 131.
37. Swearingen, J.-D., Blackwelder, R.-F. and Spalart, P.-R., Inflectional instabilities in the wall region of bounded turbulent shear flows. Report CTR-S87 (1987) pp. 291–295.
38. Tang, Y.P. and Clark, D.G., On near-wall turbulence-generating events in a turbulent boundary layer on a riblet surface. *Appl. Sci. Research* 50 (1993) 215.
39. Tardu, S., Truong, T.V. and Tanguay, B., Bursting and structure of the turbulence in an internal flow manipulated by riblets. *Appl. Sci. Res.* 50 (1993) 189.
40. Tardu, S., Feng, M.Q. and Binder, G., Quantitative analysis of flow visualizations in an unsteady channel flow. *Exp. in Fluids* 17 (1994) 158.
41. Taylor, B.-K. and Smith, C.-R., Pressure gradient effect on the development of hairpin vortices in an initially laminar boundary layer. Report FM-15, Lehigh University, Department of Mechanical Engineering and Mechanics (1990).
42. Tullis, S. and Pollard, A., A numerical investigation of the turbulent flow over V and U groove riblets using a viscous wall region model. In: So, R.M.C., Speziale, C.G. and Launder, B.E. (eds.), *Near-Wall Turbulent Flows*. Amsterdam: Elsevier (1993) pp. 761–770.
43. Tullis, S. and Pollard, A., Modelling the time dependent flow over riblets in the viscous wall region. *Appl. Sci. Res.* 50 (1993) 299.
44. Vezin, P., Tardu, S. and Binder, G., Space time organization of near wall turbulence in an unsteady channel flow. In: *International Symp. on Turbulence, Heat and Mass Transfer*, Lisboa, August (1994).
45. Vukoslavcevic, P., Wallace, J.-M. and Balint, J.-L., On the mechanism of viscous drag reduction using streamwise aligned riblets: A review with some results. In: *Proceedings on Turbulent Drag Reduction by Passive Means*. London: Royal Aeronautical Society (1987) Vol. 290.
46. Vukoslavcevic, P., Wallace, J.-M. and Balint, J.-L., Viscous drag reduction using streamwise aligned riblets. *AIAA. J.* 30 (1992) 1119.
47. Walker, J.D.A., Wall layer eruptions in turbulent flows. In: Gyr, A. (ed.), *2nd IUTAM Symp. on Structure of Turb. and Drag Reduction*. Berlin: Springer-Verlag (1989) pp. 59–67; also NASA Tech. Memo. 102362, ICOMP-89-26.
48. Walsh, M.-J., Riblets. In: Bushnell, D.M. and Hefner, J. (eds), *Viscous Drag Reduction in Boundary Layers*. Progress in Astronautics and Aeronautics, Vol. 123 (1990).